

Halogen Mediated Deinterpenetration of Interpenetrated Metal-organic Frameworks

by

Joseph Lee Strozier Jr.

Submitted in Partial Fulfillment of the Requirements

for the Degree of

Master of Science

in the

Chemistry

Program

YOUNGSTOWN STATE UNIVERSITY

May 2020

Halogen Mediated De-Interpenetration of Interpenetrated Zn Metal Organic Frameworks

Joseph Lee Strozier Jr.

I hereby release this thesis to the public. I understand that this thesis will be made available from the OhioLINK ETD Center and the Maag Library Circulation Desk for public access. I also authorize the University or other individuals to make copies of this thesis as needed for scholarly research.

Signature:

Joseph Lee Strozier Jr. Student Date

Approvals:

Douglas T Genna, Thesis Advisor Date

Christopher Arntsen, Committee Member Date

Allen D. Hunter, Committee Member Date

Dr. Salvatore A. Sanders, Dean of Graduate Studies Date

Acknowledgements

Through this long journey many people have graciously helped me from my undergraduate days to where I am now, and I'm sure I wouldn't have gotten as far without them.

I would first like to thank Dr. Sherri Lovelace-Cameron. From the go you've always had my back, checking on me and giving me advice whenever I was troubled. It was an honor taking classes and learning from you. Thank you for all the help over the years.

The other two members of my committee, Dr. Allen D. Hunter and Dr. Chris Arntsen, out of all the chemistry staff I actually haven't taken any classes from the two of you which is a shame cause both of you seem like really cool professors to learn from.

I would also like to thank Dr. Peter Norris for kicking this whole ride off. It was your organic chemistry class that made everything click and made me pursue chemistry. I loved your energy when teaching you've made every class engaging and fun. I remember when chemistry classes didn't have homework that was required like it is now but you always tried to give us the means to pass providing us with practice test and video recording of mechanism and lectures (long live hyperconjugation/peter-norris.com). Thanks for all of your advice and knowledge given to me over the years.

Of course I couldn't leave without mentioning my mentor Dr. Douglas T. Genna. Words cannot express the gratitude I feel when you accepted me into the Genna lab. Thank you

for having faith in me when I didn't have faith in myself and giving me confidence when it was wavering. Your knowledge and enthusiasm for chemistry made learning really enjoyable. My time in the advanced organic classes and organometallics classes have helped me tremendously. Remember that one time I cried when giving a literature presentation in advanced organic after that class I haven't cried in front of a crowd since (knocks on wood). You're a wonderful professor and an even better person. I will carry your teachings with me as I move on from YSU with pride. And remember it's not how you start it's how you finish, and I think I finished pretty well. Thank you for everything Professor Genna.

Can't forget the past and current members of the Genna lab. Although our time may have been short, the many adventures and good times we shared will stay with me for the years to come. Swan, Emily and Saidah I hope you all achieve everything you set out to do I wish you the best of luck in any efforts or journeys that you may pursue from this point forward. Sarah, Joseph, and Alissa you all have helped me in some manner during my stay and I'm convinced I wouldn't have made it as far without any of you. My wish is for every single one of you to prosper and succeed in whatever direction life takes you.

Thank you for the wonderful memories.

I would also like to thank my Family, my mother, father and sisters for encouraging me through every step of my journey and for their continued support in the future, especially when I was acting difficult. You all are my backbone and rock, thank you for instilling the values that made me the man I am today. I love you all dearly.

Of course the chemistry department staff, Lisa Devore, Tim Styraneć, and Ray Hoff your help has been invaluable throughout the years. Thank you for everything. And last I would like to thank my various friends I made throughout the years

ABSTRACT

The synthesis of non-functionalized IRMOF-10 is difficult due to the requirement for highly dilute conditions to prevent interpenetration. Here I report the synthesis of IRMOF-10 via the halogen mediated deinterpenetration of IRMOF-9. Although powder X-ray data is insufficient to differentiate between the MOFs IRMOF-9 and IRMOF-10 the transformation has been confirmed through additional means such as size exclusion dyeing, where one dye will be incorporated into one MOF and not the other, and density separation. Additionally, the role of different preparations of IRMOF-9 was studied, where I compare different syntheses of IRMOF-9 to see if there would be any changes when deinterpenetrating to IRMOF-10. Lastly the deinterpenetration of MOF-14 to MOF-143 was attempted.

Table of Contents	
Title Page	i
Signature Page	ii
Acknowledgements	iii
Abstract	vi
Table of Contents	vii
List of Figures	vii
List of Tables	viii
List of Schemes	viii
Introduction	
Metal Organic Frameworks.....	1
MOF-5.....	2
Interpenetration.....	3
Background of IRMOF-9/IRMOF-10.....	7
Project Background.....	9
Results and Discussion	
Synthesis of IRMOF-9 and conversion to IRMOF-10.....	12
Characterization of IRMOF-9/IRMOF-10.....	14
Synthesis of IRMOF-10.....	20
Timed experiments.....	21
Determination of 4, 4'-biphenyldicarboxylic acid and zinc content in IRMOF-9.....	24
MOF-14/MOF-143.....	32
Conclusion.....	35
References.....	46
List of Figures	
Figure 1 MOF overview.....	2
Figure 2 MOF-5.....	3
Figure 3 Overview of void space.....	4
Figure 4 MOF interpenetration.....	4
Figure 5 Overview of IRMOF-9/IRMOF-10.....	8
Figure 6 Diagram of IRMOF-9 showing 2 separate frameworks that make up the MOF.....	9
Figure 7 ATF-1 rearrangement into YCM-21-TEA.....	10
Figure 8 Proposed mechanism for arrangement of ATF-1 to YCM-21-TEA.....	11
Figure 9 Proposed mechanism for IRMOF-9 to IRMOF-10 conversion.....	12

Figure 10 Conditions for the IRMOF-9 to IRMOF-10 transition.....	13
Figure 11 PXRD patterns of IRMOF-9 in blue and IRMOF-10 in orange.....	14
Figure 12 Illustration of Reichardt's dye and Rodamine b being incorporated into MOFs.....	15
Figure 13 Rodamine b incorporated into IRMOF-9 and IRMOF-10.....	16
Figure 14 IRMOF-9/IRMOF-10 with Reichardt's dye incorporation.....	17
Figure 15 PXRD of calculated and experimental IRMOF-9/-10 IRMOF-10.....	18
Figure 16 Separation and dye test with IRMOF-9 and IRMOF-10.....	19
Figure 17 Hupp IRMOF-9/10 after dying with Reichardt's dye.....	21
Figure 18 Crystal quality of IRMOF-9/IRMOF-10.....	22
Figure 19 Timed deinterpenetrations of IRMOF-9.....	22
Figure 20 Timed deinterpenetrations of IRMOF-9 at 0.16 M & 0.25M concentrations.....	23
Figure 21 Timed deinterpenetrations of IRMOF-9 with Acetonitrile as solvent.....	23
Figure 22 Reichardt's inside IRMOF-10.....	24
Figure 23 Core shelling example.....	24
Figure 24 IRMOF-9/IRMOF-10 being measured on a ruler.....	25
Figure 25 ¹ H NMR of deinterpenetrated mother liquor and 4,4' biphenyldicarboxylic acid.....	26
Figure 26 IRMOF-9 mother liquor forming inorganic zinc.....	27
Figure 27 UV-Vis graph of IRMOF-9.....	28
Figure 28 TGA of IRMOF-9 and IRMOF-10.....	29
Figure 29 MOF-14 copper paddlewheel SBU.....	32
Figure 30 Calculated PXRD patterns of MOF-14 and MOF-143.....	33
Figure 31 Timed deinterpenetrations of MOF-14.....	34
Figure 32 Picture of MOF-14 as is and dyed with Reichardt's dye.....	34

List of Tables

Table 1 % weight loss in 24 hours.....	30
Table 2 % weight loss in a week.....	30

List of Schemes

Scheme 1 Synthesis of IRMOF9.....	36
Scheme 2 Conversion of IRMOF-9 to IRMOF-10.....	37
Scheme 3 Synthesis of IRMOF-10.....	38
Scheme 4 Synthesis of IRMOF-9 (Method #1).....	39
Scheme 5 Synthesis of IRMOF-9 (Method #2).....	40
Scheme 6 Synthesis of MOF-14.....	41
Scheme 7 Conversion of MOF-14 to MOF-143.....	42

Introduction

Metal Organic Frameworks

Metal-Organic Frameworks (MOFs) are defined as highly porous, interconnected, crystalline structures that contain metal clusters or metal ions, known as a node, that coordinate to polydentate organic ligands, known as linkers.¹ **Figure 1** shows IRMOF-9, a three-dimensional MOF that is formed by coordinating the tetra-zinc oxide (metal cluster/node) secondary binding unit (SBU) to 4,4'-biphenyldicarboxylic acid (organic linker). IRMOF-9 was synthesized by the Yaghi group in 2002 as one MOF in a series of frameworks that have structures based on the skeleton of MOF-5.²

Now the reason MOFs are so highly regarded for research purposes is that MOFs are highly tunable leading to large surface areas, modifiable functionality and high porosity. Notably the IRMOF series in particular is known for having high porosity. MOF synthesis is operationally simple often times only requiring dissolution of both metal source and ligand in a solvent and placing it in an oven. These characteristics along with the varying degree of versatility and variability of its inorganic and organic constituents make MOFs an area of interest for potential applications in gas storage and separation,³⁻⁶ catalysis,⁷⁻⁸ drug delivery⁹⁻¹⁰ and many others.¹⁰⁻¹¹

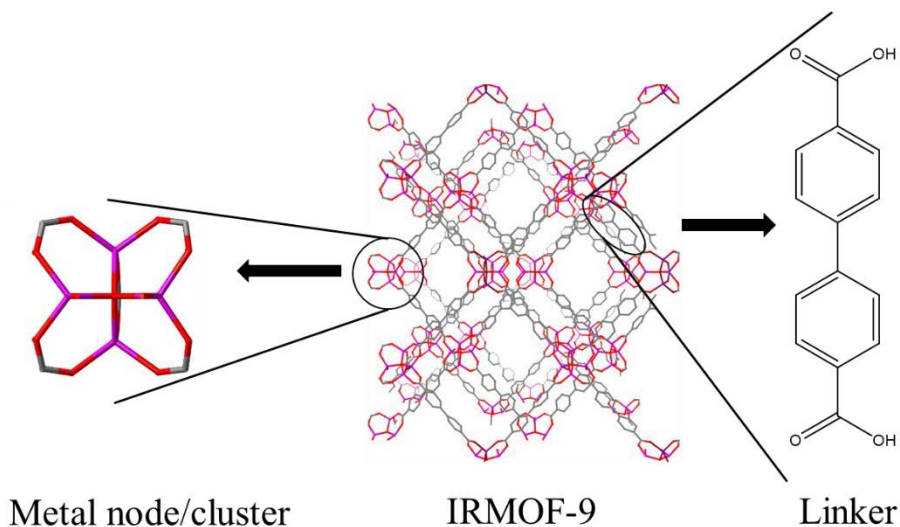


Figure 1: MOF overview

MOF-5

The Isoreticular Metal Organic Frameworks (IRMOFs), are a series of MOFs that have the same cubic network topology as MOF-5 (IRMOF-1). The conditions to synthesize the IRMOF series are similar to that of MOF-5, except that different linkers and concentrations are used, from that IRMOF-2 – IRMOF-16 can be synthesized with increasing void space. MOF-5 is a highly porous MOF made with terephthalic acid linkers connected to a tetrazinc oxide secondary building unit (SBU) leading to a structure with cubic topology (**Figure 2**). It was first synthesized by Yaghi et al, and demonstrated unique robustness in that upon evacuation of the guest solvent MOF-5 retained its morphology and crystallinity.¹² The rigid state of both its metal SBU and linker allowed the realization of isoreticular framework synthesis. The IRMOFs are a series of MOFs that have the same cubic network topology but vary in the linkers that connect the octahedral Zn_4O SBUs. Synthesis of these IRMOFs is an easy task usually involving other ditopic carboxylate linkers under close, near indistinguishable conditions.¹ While much research has been done on the IRMOF series the primary focus discussed herein will look at IRMOF-9 and IRMOF-10,

representing the interpenetrated and non-interpenetrated frameworks of the combination of the Zn_4O SBU and 4,4'-biphenyldicarboxylic acid (Figure 1).

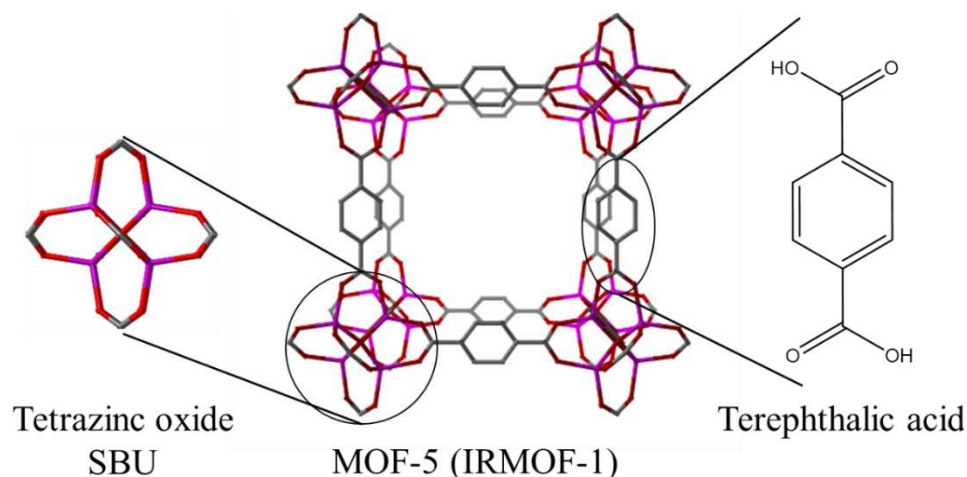


Figure 2: MOF-5

With the synthesis of MOF-5 and its ability to retain its structure after the removal of its guest solvent demonstrating permanent porosity meant that one could use MOFs to store a wide array of gas molecules.¹² While there are myriad ways to synthesize MOFs, one of the most common is through solvothermal synthesis, where the metal cluster/ion and linker are dissolved in a non-aqueous solution and heated. The synthesis of MOFs also can be realized through hydrothermal and solvent free conditions.¹³

Interpenetration

When a MOF is synthesized it creates a void space, this void space is filled with either the solvent it was grown in or a charged ion. When the linker used to create the MOF is small (ex. terephthalic acid) the MOF is stable and there is no risk of collapse. The situation changes when the linker grows in length creating a domino effect where the pores of the MOF grow in length therefore increasing the void space associated with it. When the void space becomes too large the guest molecule (solvent / charged ion) does not take up as much space. (Figure 3). This extra space introduces instability to the MOF risking collapse

of the framework. One way MOFs prevent collapse from too much void space is to introduce a second net to fill the void. (**Figure 4**).

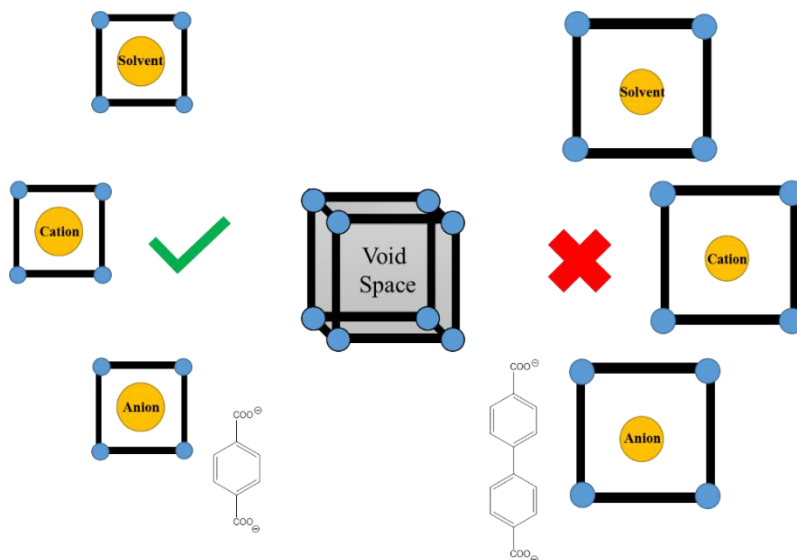


Figure 3: Overview of void

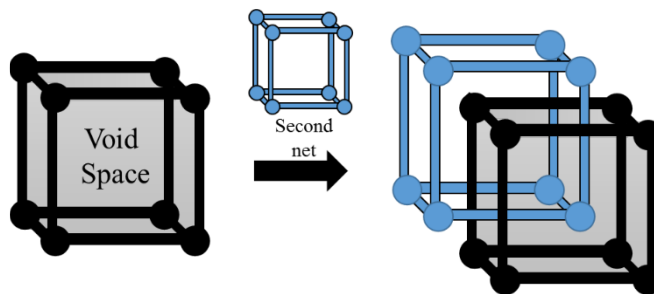


Figure 4: MOF interpenetration

This introduction of a second net is called interpenetration and synthesis of large pored non-interpenetrated MOFs is still a formidable task due to the thermodynamic favorability that interpenetration provides (i.e. nature abhors a vacuum). For example, it was found in the IRMOF series that after a certain linker length, 1,4-biphenyldicarboxylic acid, MOFs will form as an interpenetrated structure.³ Of course, longer linkers are not the only defining factor in determining if a MOF will interpenetrate. In order to strengthen the structural stability of a MOF interpenetration occurs, as the forces between frameworks are

not chemical bonds but other interactions (π - π stacking, hydrogen bonding and van der Waals forces) that is neither tethered or connected by any covalent interaction but cannot be separated without breaking bonds.¹⁴ Although not without its own set of merits interpenetration causes an increase in a MOF's thermal stability¹⁵ and as stated above, since the frameworks themselves aren't physically connect to one another it creates a rigid environment. Interpenetrated MOFs also assist in CO₂ uptake¹⁶, due to the systemic filling of the pores, and enhance hydrocarbon storage and separation.¹⁷ The Schröder group demonstrates this uptake in CO₂ by synthesizing NOTT-202a, an indium based MOF that allows capture of gases at high pressure, but selectively leave CO₂ trapped in the pores at low pressure. This is due to one of the frameworks of NOTT-202a being partially interpenetrated and the stepwise filling of the pores. The sorption isotherms for a range of gasses (CO₂, O₂, CH₄, Ar, N₂, and H₂) were tested up to 1.0 bar through a range of temperatures. It was found that below the triple point of the CO₂ phase diagram, specifically at 195k, 205k and 213k, NOTT-202a demonstrates enhanced CO₂ adsorption and slow kinetics when external pressure decreases, while other gases, O₂, CH₄, Ar, N₂, and H₂, tested have good isotherm reversibility when the external pressure starts to drop. And at temperatures above CO₂'s triple point (5.26 bar, 216.7K) the CO₂ isotherm is fully reversible and NOTT-202a exhibits a lower uptake in CO₂.¹⁸ Of course there are drawbacks to interpenetration (decreased surface area, porosity, pore aperture and free volume).^{19,20} But these shortcomings may be beneficial for applications mentioned earlier as some may require these traits. Despite the drawbacks of interpenetration there are some MOFs that have interesting properties due to interpenetration such as this nickel based MOF synthesized by Kitagawa et al. $\{[\text{Ni}(\text{bpe})_2(\text{N}(\text{CN})_2)](\text{N}(\text{CN})_2)(5\text{H}_2\text{O})\}_n$ where (bpe

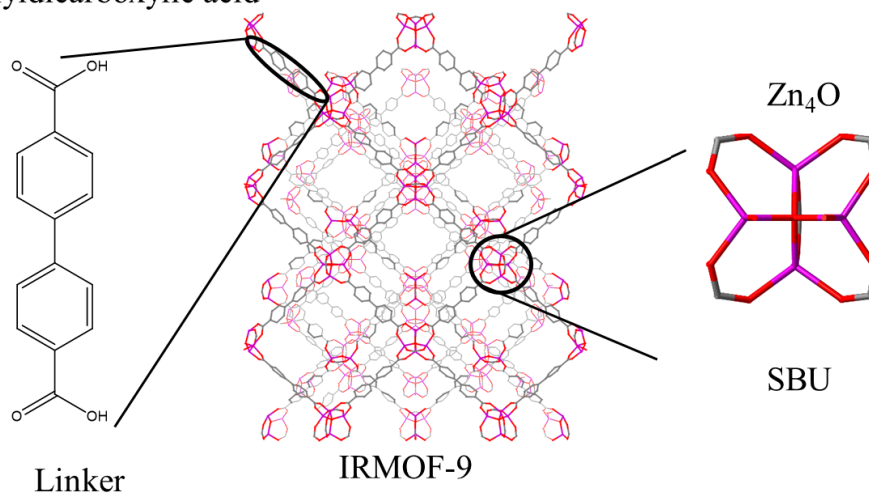
= 1,2-bis(4-pyridyl)ethane and $\text{N}(\text{CN})_2^-$ = dicyanamide) shows permanent porosity high thermal stability and highly selective sorption and anion exchange properties. Interestingly this MOF shows that there is a stepwise sorption with methanol accompanying a structural transformation from a dehydrated to guest occupied structure via X-ray powder diffraction. Also, despite adequate pore size there is no diffusion of oxygen or nitrogen into the pores at 77 K, but there is significant carbon dioxide uptake at 195 K despite its similar size to oxygen. With the synthesis of this nickel MOF there is a free dicyanamide anion in the channel due to one of the frameworks being insoluble in common solvents it was hypothesized that an anion exchange would take place. N_3^- (azide), NCO^- (cyanate), NO_3^- (Nitrate), and BF_4^- (tetrafluoroborate) were chosen due to their smaller size but only N_3^- was able to undergo the exchange.²¹ These reasons are why chemists sought ways to control the interpenetration phenomenon through careful control of temperature and concentration to ligand design and template control. Certain reaction parameters such as concentration and temperature are shown to be paramount in controlling MOF interpenetration. For example, more dilute reaction conditions favor the formation of non-interpenetrating MOFs with larger pores. As shown when Yaghi *et al* synthesized the IRMOF series. IRMOFs-9, -11, -13 and -15 are all 2-fold interpenetrated structures; however, by carrying out their original syntheses under more dilute conditions their non-interpenetrated versions, IRMOFs-10, -12, -14 and -16, could be realized.¹ Temperature is also a means to control interpenetration as seen when Qiang Xu *et al* went on to synthesize a nonporous, 2-fold interpenetrated MOF ($\text{Cd}(\text{abdc})(4,4' \text{-bpy})$) and only by lowering the temperature from 160 °C to 105 °C could the microporous, non-interpenetrated MOF ($\text{Cd}(\text{abdc})(4,4' \text{-bpy}) \cdot 4\text{H}_2\text{O} \cdot 2.5\text{DMF}$) be obtained.²² Another way to deter interpenetration is to use a

template and have the MOF self-assemble around it as the template would fill that void space. The Zhou group demonstrated this when synthesizing PCN-6' from a reaction between $\text{Cu}(\text{NO}_3)_2 \cdot 2.5\text{H}_2\text{O}$ and H_3TATB in the presence of oxalic acid yielded the non-interpenetrated MOF. Whereas under the same conditions without oxalic acid would bestow the interpenetrated PCN-6.²³ There is also reversible interpenetration, where the removal of the guest solvent can cause a MOF to undergo a conformational change from a closed interpenetrated structure to an open non-interpenetrated structure. The Kim group exemplified this when upon the activation of MOF-123, where DMF was evacuated from the pores converted non-interpenetrated MOF-123 to interpenetrated MOF-246.²⁴ The catenated structure makes up for these limitations by becoming more robust by increasing wall thickness and reducing pore size.^{25,26} Although interpenetration has its own shortcomings such as decreased surface area, porosity etc. There are also plenty of benefits such as increased small molecule selectivity²⁷ enhanced gas storage, thermal stability.

Background of IRMOF-9/IRMOF-10

The majority of the research reported in this thesis is on IRMOF-9/-10. IRMOF-9 is a doubly interpenetrated structure with a Zn_4O octahedral SBU linked by 4,4' biphenyldicarboxylate (**Figure 5, Figure 6**). The surface area of IRMOF-9 measures $\sim 1900 \text{ m}^2/\text{g}$.²⁸ IRMOF-10 is the non-catenated form of IRMOF-9, both MOFs are comprised of the same SBU and linker (**Figure 5**). IRMOF-10 has a theoretical surface area of about $5000 \text{ m}^2/\text{g}$.²⁹ While the crystal structure of IRMOF-9 has been solved, a crystal structure of non-functionalized IRMOF-10 is all but latent. All reported structures of IRMOF-10 are only simulations derived from IRMOF-12.¹

4,4'-Biphenyldicarboxylic acid



4,4'-Biphenyldicarboxylic acid

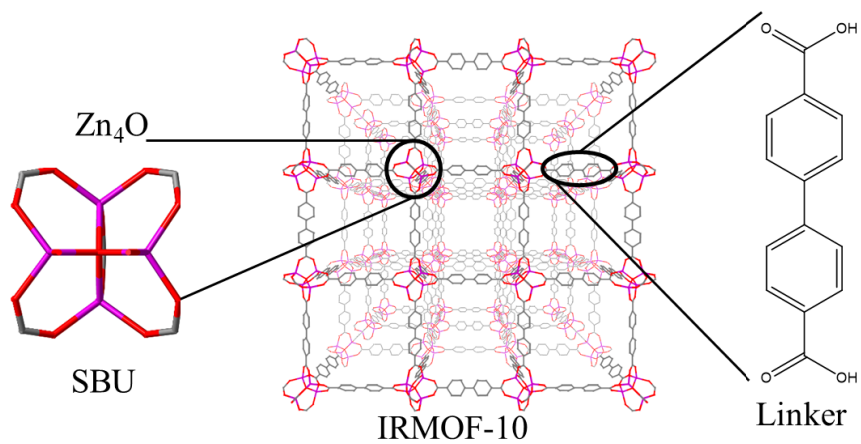


Figure 5: A) Overview of interpenetrated IRMOF-9 with 4,4'-biphenyldicarboxylic acid linker and a tetrazinc oxide SBU. B) Overview of non-interpenetrated IRMOF-10 with 4,4'-biphenyldicarboxylic acid linker and a tetrazinc oxide SBU

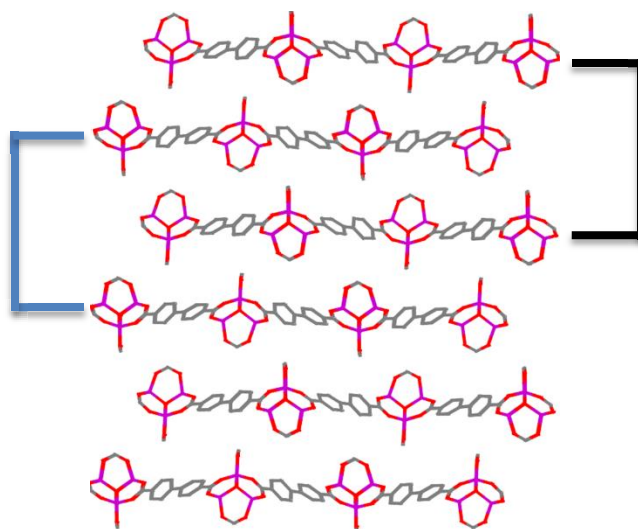


Figure 6: Diagram of IRMOF-9 showing 2 separate frameworks that make up the MOF

Project background

The inspiration for this project is based on work done by M. K. Bellas and J. J. Mihaly, where they transformed the three dimensional MOF, ATF-1, via the use of tetraethylammonium salts, to a two dimensional MOF, YCM-21 (YCM = Youngstown Crystalline Material) as seen in **Figure 7**. Initially ATF-1 was treated with a 0.08 M solution tetraethylammonium bromide in DCM and within a week partial conversion of ATF-1 to YCM-21 was observed. And after ATF-1 was treated with a 0.16 M solution of tetraethylammonium bromide (TEABr) in DMF it underwent the full transformation in 24 hours at 120 °C. Of note was the importance of a nucleophilic counterion, the use of dichloromethane and temperature. A non-nucleophilic counter would not allow the reaction to take place as would running the reaction in the absence of DCM at room temperature. Even the case of dissolving ATF-1 using TEABr in DMF yielded no reaction at room temperature, with minimum conversion being reached after adding as little as 1 equivalent of DCM with full conversion requiring 49 equivalents. The transformation will

also occur at temperatures as low as 80 °C with 120 °C as the optimal temperature for the transformation. Except in the case when ATF-1 was suspended in 0.16 M solutions of tetraethylammonium chloride (TEACl) in DMF or TEABr in DMF/CH₂Cl₂. Where it was observed that the framework was dissolved in 24 hours but treating ATF-1 with just TEABr in DMF at 120 °C one would see complete conversion to YCM-21.

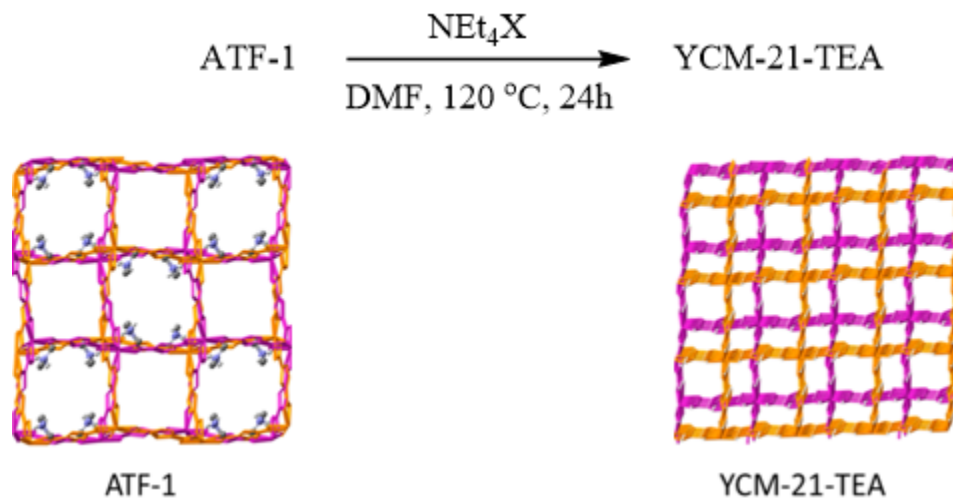


Figure 7: ATF-1 rearrangement into YCM-21-TEA²⁷

The proposed mechanism for this transformation is predicated on a reversible nucleophilic attack by a halide that would lead to cleavage of the In-carboxylate bond of one of the interpenetrated frameworks forming an interim SBU, [In(CO₂R)₃Br]⁻. At this point the new intermediate framework would then deinterpenetrate from its sister framework with assistance from the cation exchange. Afterwards the carboxylate would rebound displacing the bromine and the two frameworks would then be separated and this would continue until the entire interpenetrated MOF frameworks were separated (**Figure 8**).³⁰

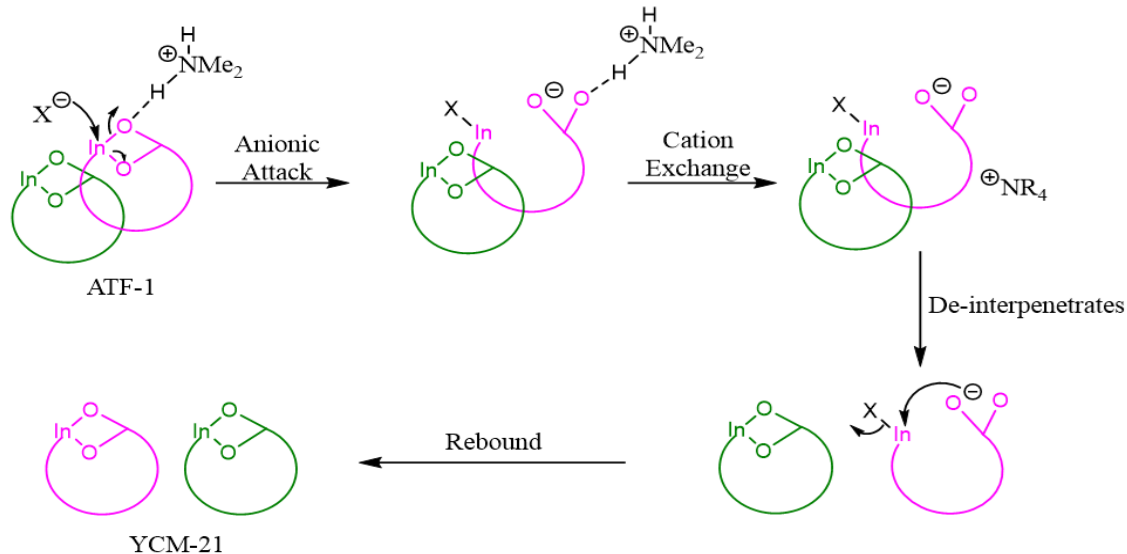


Figure 8: Proposed mechanism for arrangement of ATF-1 to YCM-21TEA

We wanted to see if that same rearrangement would take place in the IRMOF-9 framework with the ZnO_4 SBU. A similar mechanism for the ATF-1 to YCM-21 conversion was proposed with a slight modification. **Figure 9** proposes a possible mechanism for the transformation, where a reversible nucleophilic attack by a counter ion would lead to the cleavage of the zinc carboxylate bond of one of the interpenetrated frameworks. That framework would then deinterpenetrate from its sister framework, afterwards the carboxylate would rebound displacing the halide and the two frameworks would then be separated. Seeing as IRMOF-9 is a neutral framework there would be no cation exchange to assist with deinterpenetration.

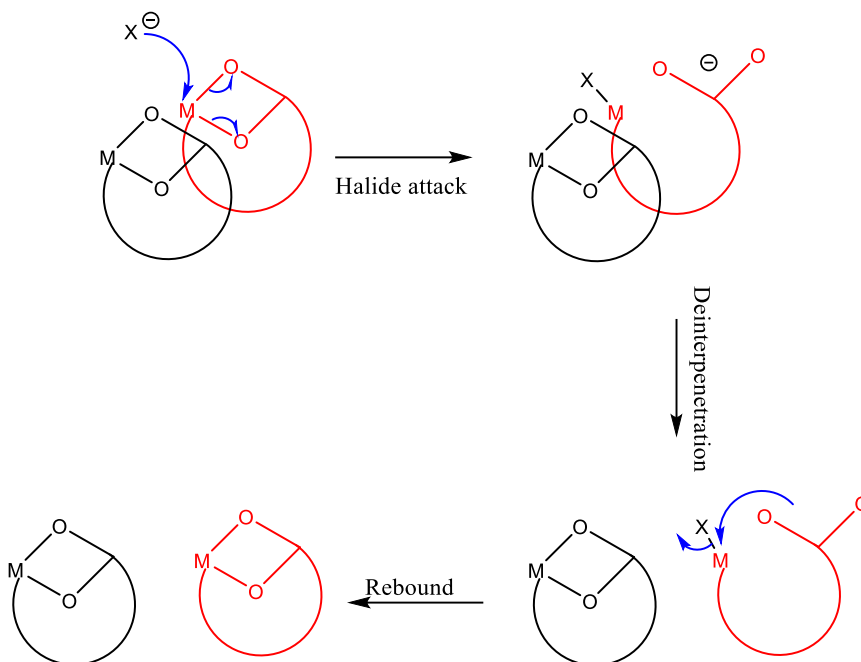


Figure 9: Proposed mechanism for IRMOF-9 to IRMOF-10 conversion.

Results and Discussion

Synthesis of IRMOF-9 and conversion to IRMOF-10

Initial efforts were first put into synthesizing IRMOF-9 which was prepared according to literature.² Where $\text{Zn}(\text{NO}_3)_2$ (6.9 mmol) and 4,4'-biphenyldicarboxylic acid (1.2 mmol) were dissolved in DMF and solvothermal synthesis at 100 °C for 24 hours yielded IRMOF-9. IRMOF-9 is a doubly interpenetrated neutral framework with an octahedral SBU geometry. Research efforts then shifted to converting IRMOF-9 to IRMOF-10, It is known that synthesis of the non-interpenetrated forms of IRMOF-9, -11, -13 and -15 require carrying out the original reaction under more dilute (and low yielding) reaction conditions. We hypothesized that subjecting IRMOF-9 to similar conditions used in converting ATF-1 to YCM-21, would IRMOF-9 lead to a similar deinterpenetration transformation. IRMOF-9 was subjected to a DMF (1 mL), 0.32M halide mixture (1 mL) (1.0g of tetraethylammonium bromide dissolved in 15 mL of dichloromethane = halide mixture),

that was allowed to deinterpenetrate on an orbital shaker at room temperature for 24 hours. After which the MOF is washed with fresh DMF and IRMOF-10 would be afforded (**Figure 10**). Other tetraethylammonium salts (TEACl and tetraethylammonium iodide, TEAI) were used to optimise the deinterpenetration but when it came time to dye the MOFs that set in these corresponding solutions the TEAI in DCM did not facilitate in the transition of IRMOF-9 to IRMOF-10. Whereas while the TEACl in DCM did help convert IRMOF-9 to IRMOF-10 the conversion was inconsistent. A key challenge in this chemistry is that both IRMOF-9 and IRMOF-10 have nearly identical PXRD patterns (**Figure 11**). Which raises the question how would one go about characterizing and distinguishing the two IRMOFs. This would require the development of additional characterization methods to differentiate the two frameworks.

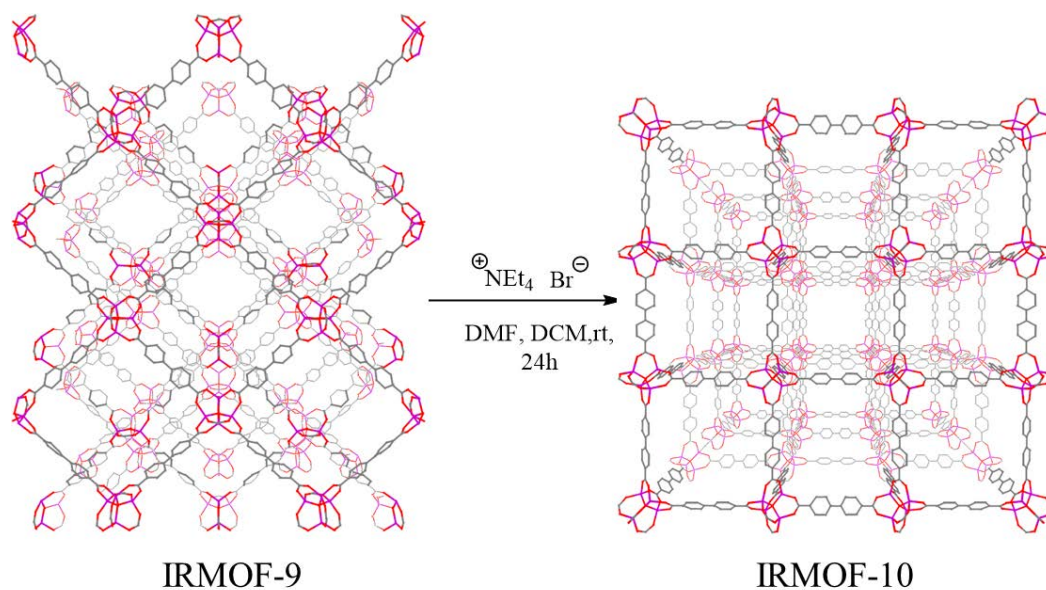


Figure 10: Conditions for the IRMOF-9 to IRMOF-10 transition.

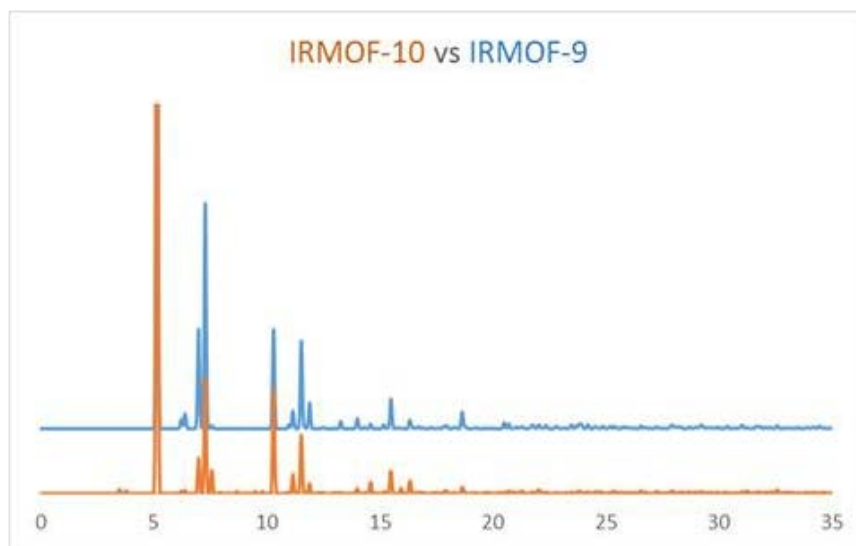


Figure 11: PXRD patterns of IRMOF-9 in blue and IRMOF-10 in

Characterization of IRMOF-9/IRMOF-10

In 2008 Hupp reported the separation of IRMOF-9 from IRMOF-10 by density using a 4:5:26 (b/v) solution of CH_2Cl_2 : CHCl_3 : CH_2BrCl . In this solution IRMOF-10 would float while IRMOF-9 would sink.³¹ We hypothesized that this technique could be used to differentiate samples of IRMOF-9 and IRMOF-10; however, it was deemed that a second complementary technique would be needed to fully characterize the two materials. To this end, we turned our attention to the apertures of IRMOF-9 and IRMOF-10. The pore aperture of IRMOF-9 should be smaller than that of IRMOF-10, 8.1Å/10.7Å for IRMOF-9 vs 16.7Å/20.2Å for IRMOF-10. Meaning that we can use a dye as a guest molecule to distinguish between the two MOFs. The idea is to choose two dyes, one that will be able to go into both IRMOFs and another dye that will only be able to fit into the IRMOF with the larger opening as demonstrated in **Figure 12**.

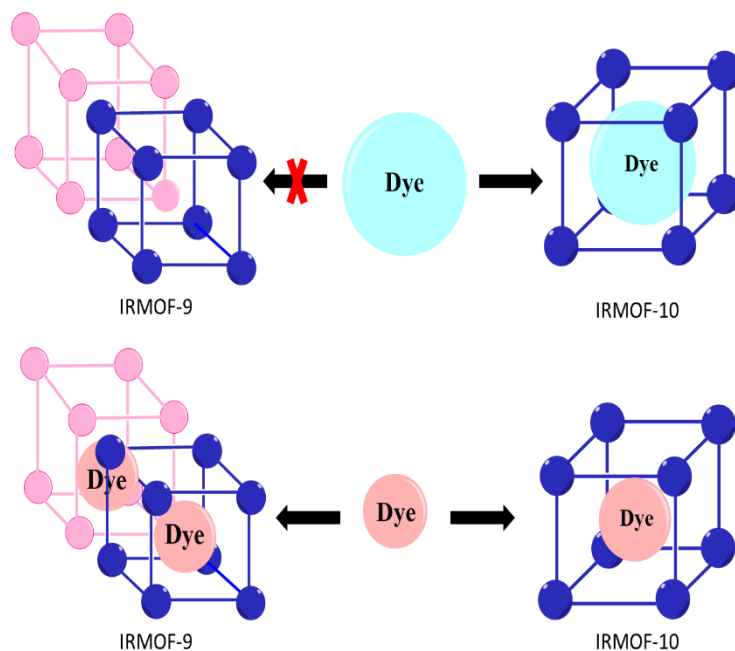


Figure 12: Illustration of Reichardt's dye (light blue ball) moving inside the void space of IRMOF-10 and being too large to be incorporated into IRMOF-9. B) Rhodamine b (salmon ball) being incorporated into both IRMOF-9 and IRMOF-10

Rhodamine-b was our first choice to use as a standard as its structure is small enough that it is able to be incorporated into both IRMOF-9 and IRMOF-10. Both IRMOF-9 and IRMOF-10 were placed in separate 4 mL vials submerged in a solution containing Rhodamine B dissolved in DMF for 24 hours. Afterwards one would see bright pink crystals for both IRMOF-9 and IRMOF-10 after removal from the dyeing solution (**Figure 13**).

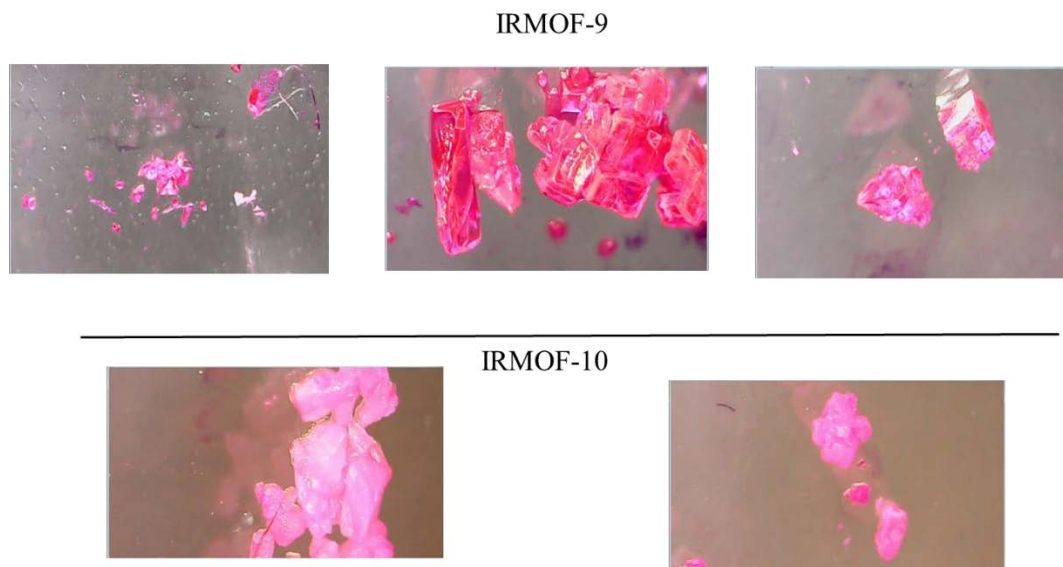


Figure 13: Rhodamine b incorporated into IRMOF-9 and IRMOF-10.

With confirmation that Rhodamine B goes into both IRMOF-9 and IRMOF-10 the next step was to find a dye that would fit into the non-catenated IRMOF-10 and reject IRMOF-9. Reichardt's dye was chosen as the dye to differentiate between the two IRMOFs. Both IRMOFs were again placed in separate 4 mL vials submerged in a solution containing Reichardt's dye dissolved in DMF for 24 hours. After the allotted time has passed one would observe that IRMOF-9, after excess DMF has been removed, did not incorporate Reichardt's dye leaving the crystal clear and colorless. Contrast that to IRMOF-10 where after removal of excess DMF one would observe a deep forest green crystal showing incorporation of Reichardt's dye into the framework (**Figure 14**). The juxtaposition of these two IRMOFs show that we can now differentiate between the two via a simple dye test.

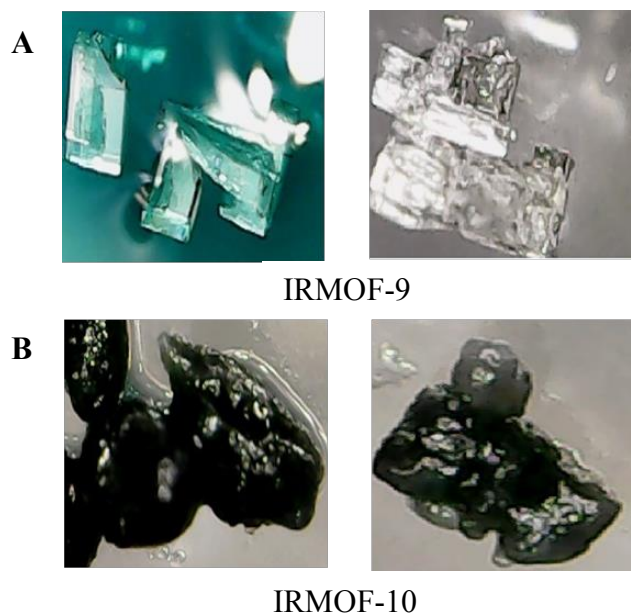
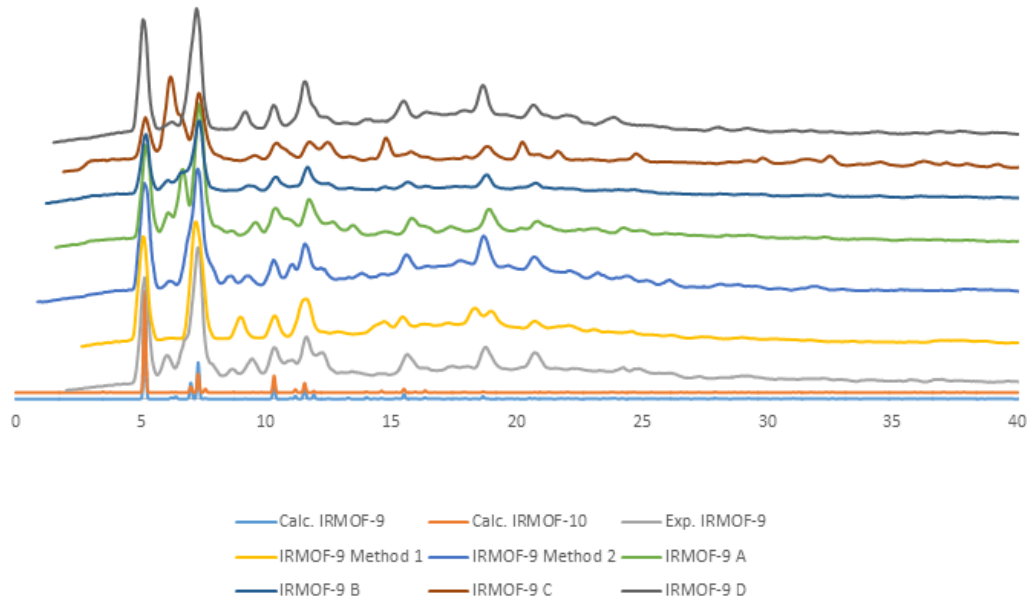


Figure 14: A) IRMOF-9 showing no Reichardt's dye uptake. B) IRMOF-10 with Reichardt's dye incorporation.

The next step was to see if the observable results (separation by density and dye incorporation) would persist with other synthesis methods of IRMOF-9 and to what extent it would have in their conversion to IRMOF-10.

All initial IRMOF-9 samples were prepared as described by Yaghi.^{31,32} The experiments performed all share the same results, the fact that the observable powder patterns for IRMOF-9 and IRMOF-10 are completely indistinguishable from one another (**Figure 15**).

Calculated IRMOF-9/-10 vs Experimental IRMOF-9



Calculated IRMOF-9/-10 vs Experimental IRMOF-10

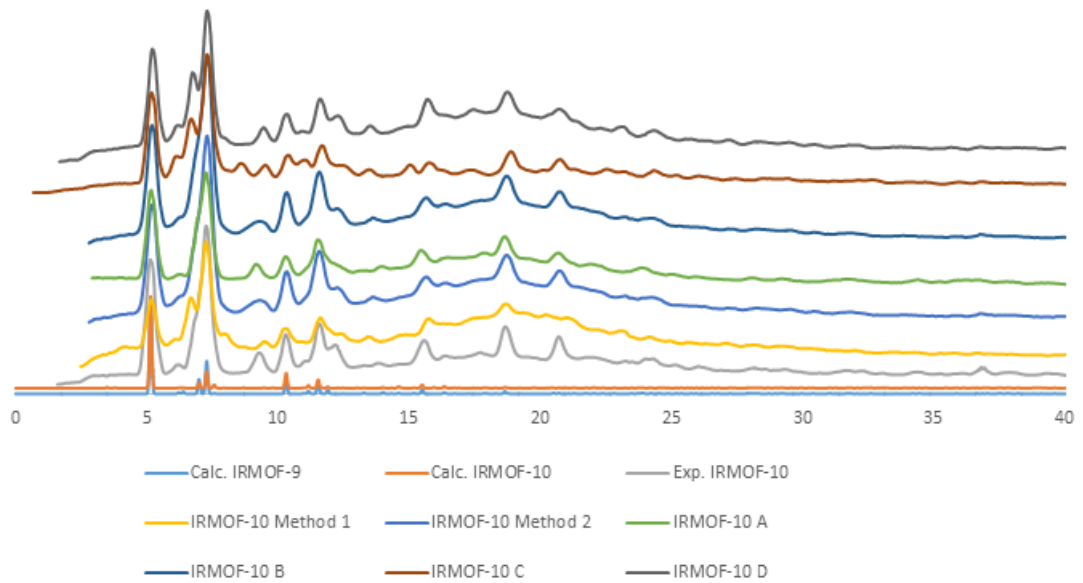


Figure 15: PXRD of calculated IRMOF-9 and IRMOF-10 compared to experimental IRMOF-9 (Top) and IRMOF-10 (Bottom)

All IRMOF-9 and IRMOF-10 samples incorporated Rhodamine b into their framework, while only IRMOF-10 could incorporate Reichardt's dye. All samples of IRMOF-9 when suspended in the separation mixture gravitated towards the bottom and the IRMOF-10 samples floated at the top (**Figure 16**). TGA curves of IRMOF-9 were stable between 200 °C and 400 °C while the TGA curve of IRMOF-10 continuously degraded.

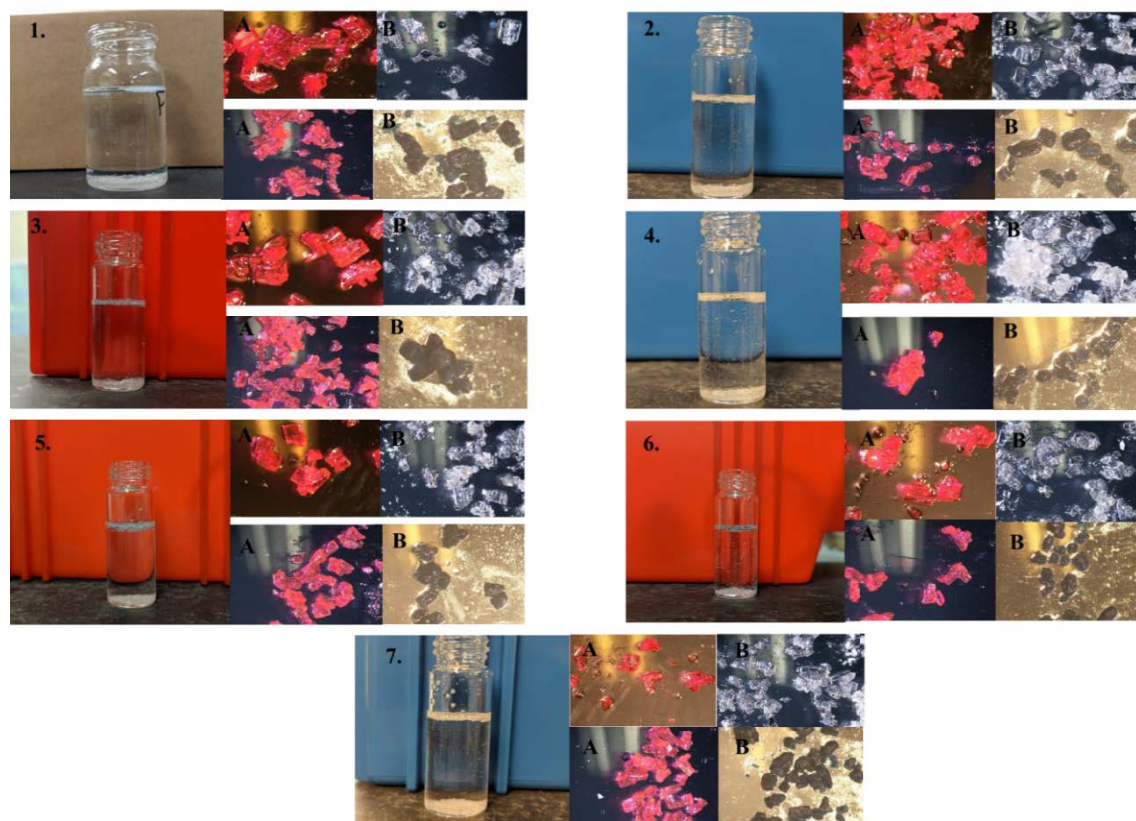


Figure: 16: 1-7 IRMOF-9 and -10 pictured in a vial with IRMOF-9 at the bottom and IRMOF-10 floating. **1-7A:** IRMOF-9 and -10 dyed with Rhodamine B. **1-7B:** IRMOF-9 with no incorporation of Reichardt's dye on top with IRMOF-10 dyed with Rhodamine B on the bottom.

Synthesis of IRMOF-10

Following the successful characterization of IRMOF-9, the focus then moved to the synthesis of IRMOF-10. Admittedly there are few experimental studies done on direct solvothermal synthesis of non-functionalized IRMOF-10, likely due to the difficulty of synthesizing the framework.^{29,31} Our efforts focused on using the conditions reported by Eddaoudi et al for the synthesis of non-interpenetrated MOF-5.³ “An *N,N*-diethylformamide (DEF) solution mixture of $Zn(NO_3)_2 \cdot 4H_2O$ and the acid form of 1,4-benzenedicarboxylate (BDC) are heated (85° to 105° °C) in a closed vessel to give crystalline MOF-5”.³ With a change of linker to H_2BDC and under more dilute conditions IRMOF-10 can be obtained.

Through correspondence between Jeremy Feldblyum (SUNY Albany), Joseph Hupp (Northwestern University), and Douglas Genna (Youngstown State University) a method to synthesize IRMOF-10 as obtained. Where zinc nitrate hexahydrate (0.7g, 2.35mmol) and 4,4'-biphenyldicarboxylic acid (0.1g, 0.41mmol) are dissolved in 260mL of DMF and placed in the oven (100° °C) for 48 hours yielded clear cubic MOF, although not much can be determined from PXRD. Most likely the resulting MOFs are a mixture of IRMOF-9 and IRMOF-10. This was confirmed when the mixture was subjected to the 4:5:26 (b/v) solution of $CH_2Cl_2:CHCl_3:CH_2BrCl$ solvent mixture and some crystals (IRMOF-10) floated and some crystals (IRMOF-9) sank to the bottom. My recreation of this synthesis should have rewarded the same results, a vial of IRMOF-10 contaminated with IRMOF-9. To test if IRMOF-10 was actually synthesized both the floating (IRMOF-10) and sinking (IRMOF-9) MOFs were treated with Reichardt's dye. It was found that neither the floating

or sinking MOF had incorporated Reichardt's dye but after being treated with our standard deinterpenetratin conditions both were found to incorporate the dye (**Figure 17**).

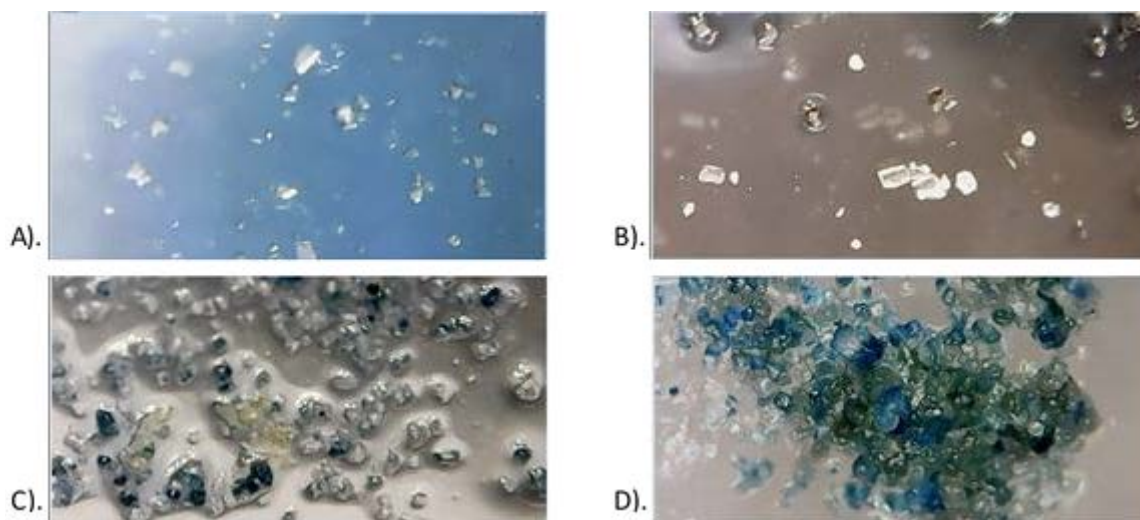


Figure 17: A) IRMOF-9 (Sinking) that did not incorporate Reichardt's dye. B) IRMOF-10 (Floating) that did not incorporate Reichardt's dye. C) IRMOF-9 after deinterpenetration with Reichardt's dye incorporation D) IRMOF-10 after deinterpenetration with Reichardt's dye incorporation.

Timed experiments

After confirming dye incorporation into IRMOF-10 it was observed that there was a noticeable drop in IRMOF-10 crystal quality after being subjected to deinterpenetration for 24 hours as seen in **Figure 18**. To preserve the crystal quality timed experiments were ran where IRMOF-9 crystals were left to deinterpenetrate for every hour, up to six hours then the reaction was arrested by washing with DMF and then treated with Reichardt's to see if the dye would incorporate into the MOF. The results show two important facts: 1) That within the first hour there is partial deinterpenetration of IRMOF-9. This is supported by IRMOF-10 having some dye incorporation at the 1 hour mark. 2) There is complete deinterpenetration at 5 hours this is also supported by IRMOF-10 being fully dyed at the 5 hours mark. (**Figure 19**). These timed experiments were also performed with 0.16 M and

0.25 M solutions to see if a decrease in concentration would improve crystal quality during deinterpenetration and substituting acetonitrile for DCM. While the crystal quality remained intact more time was need to complete the IRMOF-9 to IRMOF-10 transition (Figure 20, Figure 21). Now contrast the previous method needing 24 hours for full conversion of ATF-1 to YCM-21 at 120 °C, to my IRMOF-9 to IRMOF-10 conversion that takes only 5 hours at room temperature, and one can see a drastic decrease in time and temperature.

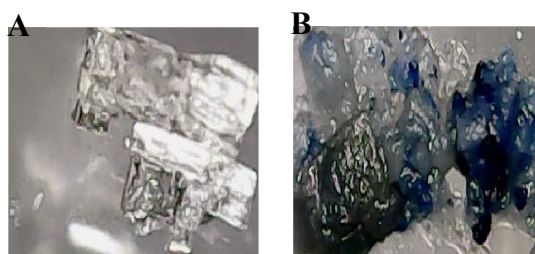


Figure 18: A) Crystalline IRMOF-9. B) IRMOF-10 with degraded crystal quality



Figure 19: Timed deinterpenetrations from 1 hour to 6 hours. Green box shows partial deinterpenetration. Red box shows complete deinterpenetration

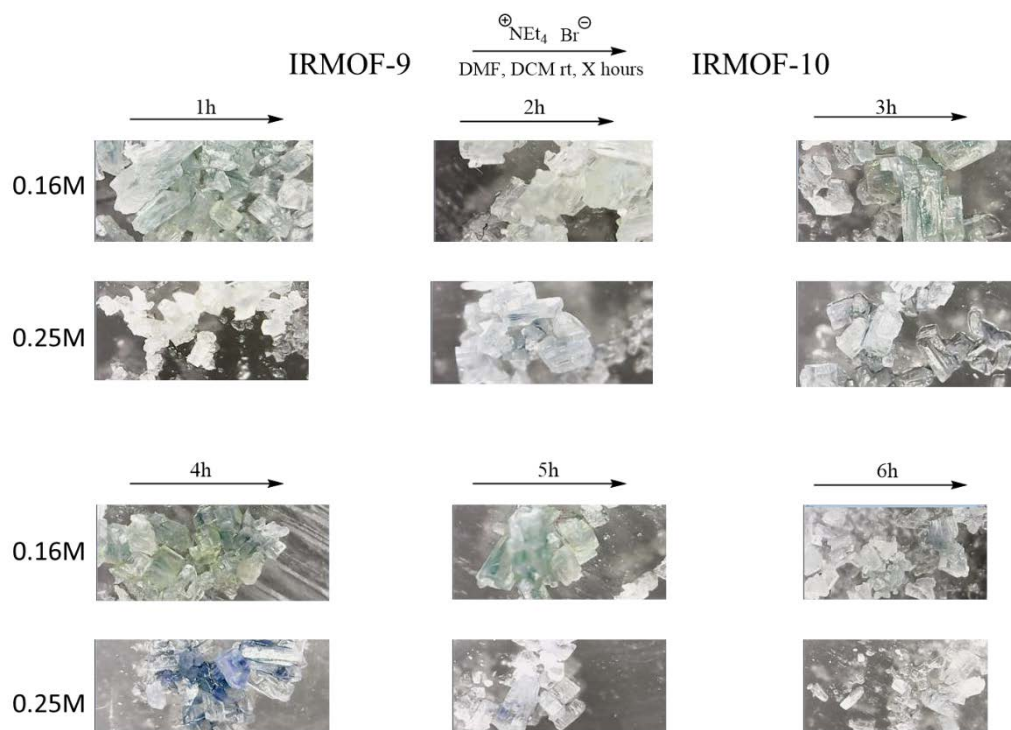


Figure 20: Timed de-interpenetrations from 1 to 6 hours at a reduced concentration

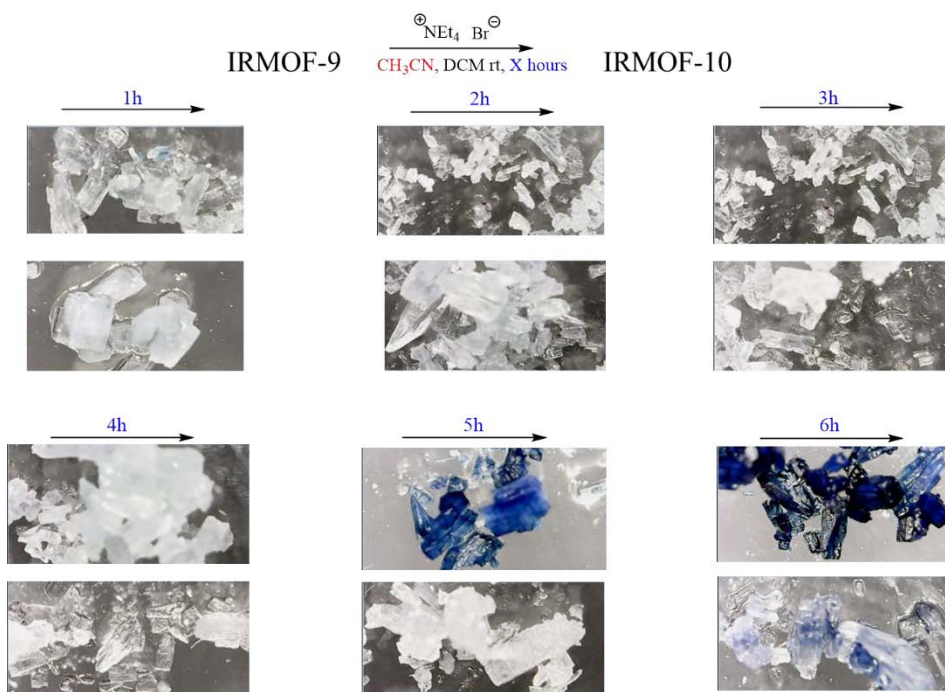


Figure 21: Timed de-interpenetrations from 1 to 6 hours with acetonitrile as the solvent

Determination of 4, 4'-biphenyldicarboxylic acid and zinc content in IRMOF-9

Following subsequent repeats of the experiment a strange phenomenon occurred where dye was observed on the inside of the crystal while the outside reminded clear and colorless (Figure 22).



Figure 22: Reichardt's dye observed on the inside of IRMOF-10

Attention was then shifted to see why this occurrence was happening with the initial hypothesis was that the IRMOF-9 was forming around IRMOF-10, or what would be called core-shelling (Figure 23). Where one can layer one MOF over another (akin to Russian tea dolls) as described by Matzger who layered MOF-5 (IRMOF-1) over IRMOF-3 by putting a seed of IRMOF-3 in a solution containing unreacted 1,4-benzenedicarboxylic acid and $Zn(NO_3)_2$.³³ With core-shelling one should see a physical difference in the MOF itself for instance the MOF expanding in size.

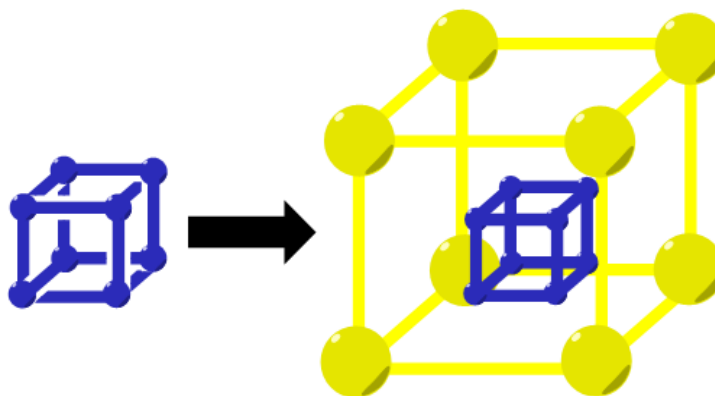


Figure 23: An example of a MOF forming (core-shelling) around another MOF.

With that in mind crystals of IRMOF-9 were measured using a centimeter marked ruler and after de-interpenetration for 5 hours were measured again. Results were inconclusive as the growth was very miniscule or there was no change at all (**Figure 24**).

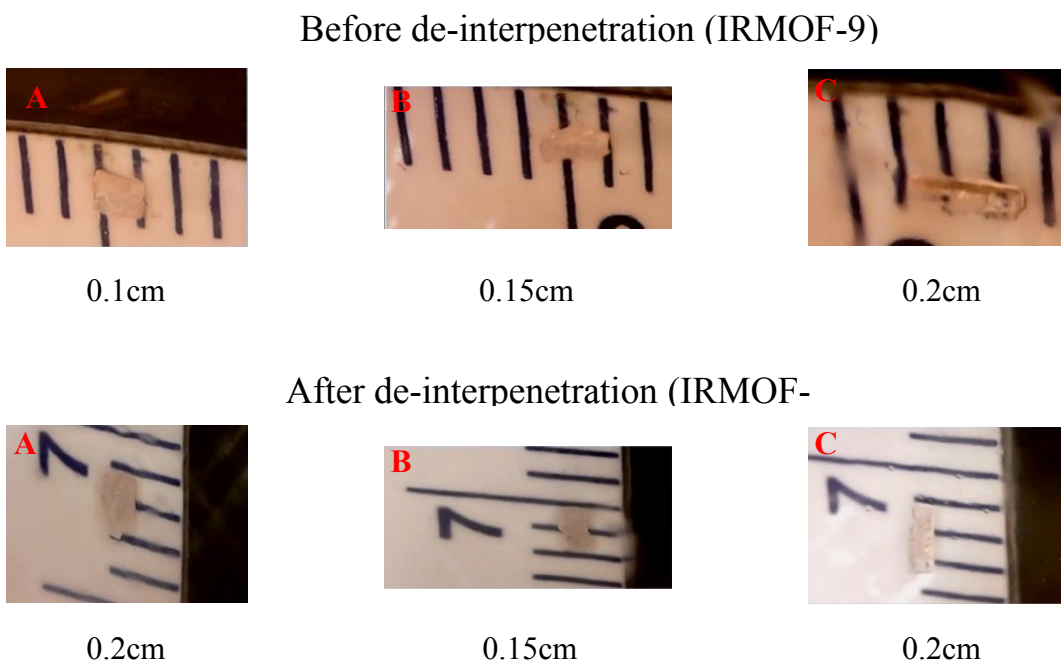


Figure 24: Crystals of IRMOF-9 and -10 shown before and after de-interpenetration being measured on a centimeter ruler

The focus of the hypothesis then shifted to one of the frameworks dissolving in solution during deinterpenetration, which would lead to the presence of 4,4'-biphenyldicarboxylic acid in the supernatant. To test this IRMOF-9 was deinterpenetrated for 5 hours after which the deinterpenetrated supernatant was transferred to another vial that was pumped under 5 mmHg of atmospheric pressure while being heated at 90 °C until the DMF was evaporated off. The resulting solid left was then dissolved in DMSO-D₆ and analyzed via ¹H NMR. Results show that 4, 4'-biphenyldicarboxylic was indeed present in the supernatant (**Figure 25**).

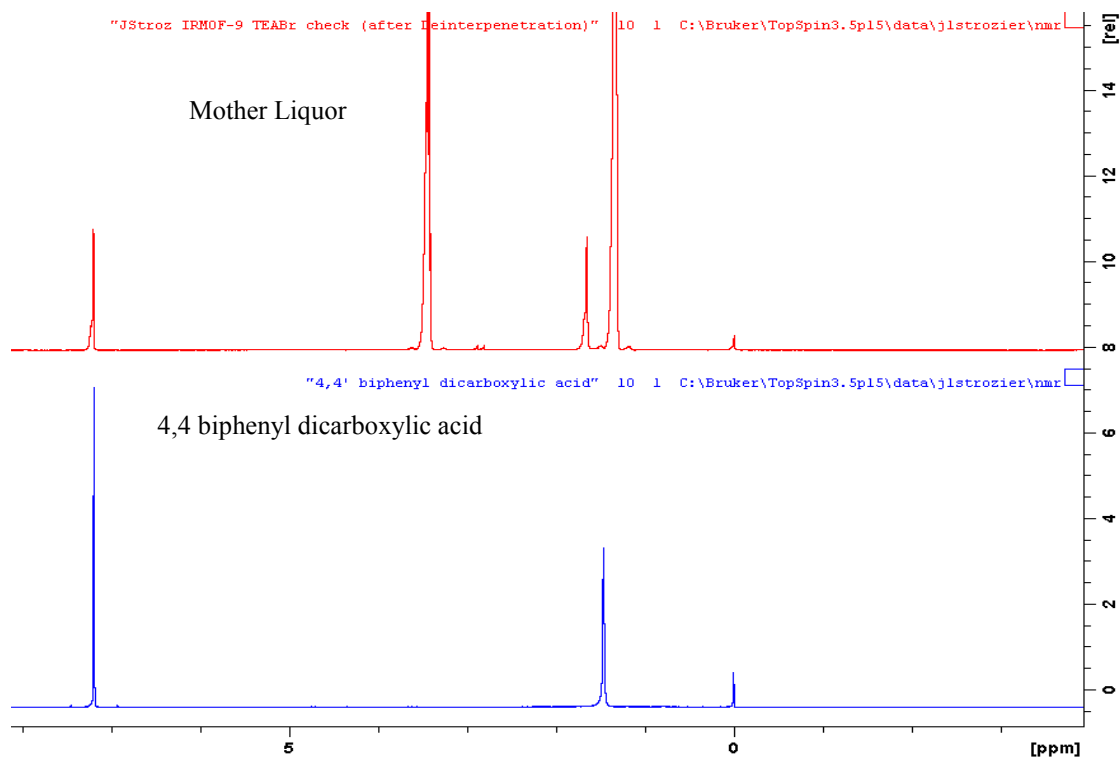


Figure 25: ^1H NMR of the mother liquor and

To complement that experiment another was run where IRMOF-9 was deinterpenetrated for 24 hours after which the supernatant was transferred to another 20 mL Teflon lined vial and heated for 7 hours, initial speculation was that if one of the frameworks of IRMOF-9 was dissolving into solution then reheating the supernatant would reform more IRMOF-9 but in less quantity. After reheating the mother liquor in a 100 °C oven for 24 hours cubic like crystals formed and were analyzed via PXRD, it was found that the crystals were a form of inorganic zinc as the powder pattern matched that of zinc nitrate (**Figure 26**).

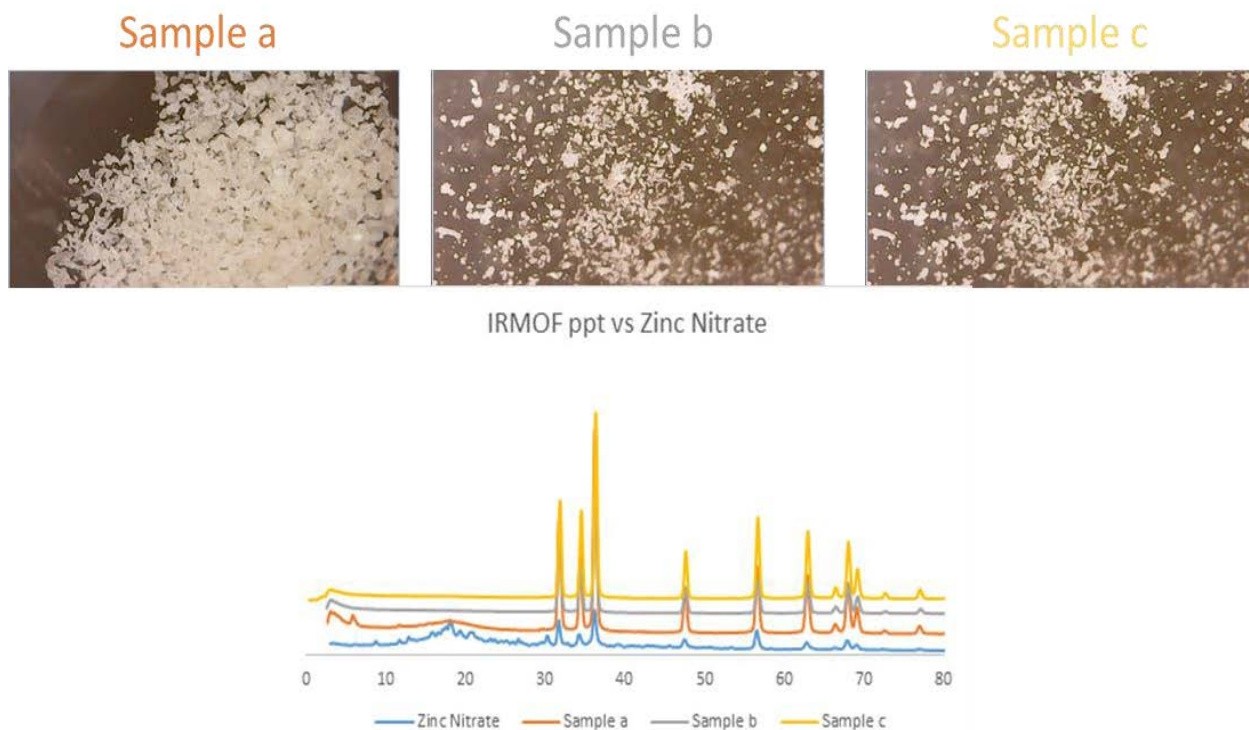


Figure 26: Samples of the IRMOF-9 mother liquor reheated in an oven forming inorganic zinc.

After successfully finding 4,4'-biphenyldicarboxylic acid in the supernatant our attention was shifted to finding the rate at which the linker was dissociating into solution using absorbance spectroscopy. It was found that as soon as IRMOF-9 was added to the pre-mixed halide solution, 4,4'-biphenyldicarboxylic acid is immediately present in solution and within 10 minutes the detector is maxed out (**Figure 27**). In totality, the NMR, PXRD, and UV-vis data led to the conclusion that one of the frameworks of IRMOF-9 is dissolving. This was further supported by measuring the mass change, if any, in the MOF during the deinterpenetration experiment. This change can be determined simply by using an analytical lab balance combined with Thermalgravimetric Analysis (TGA). The balance is used to get the initial weight of the MOF after it has been dried under vacuum at room temperature for 24 hours.

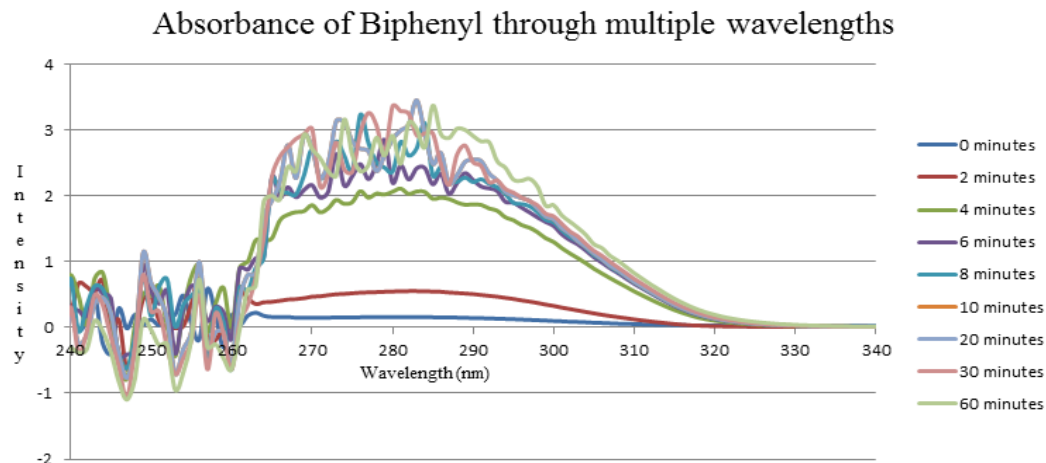


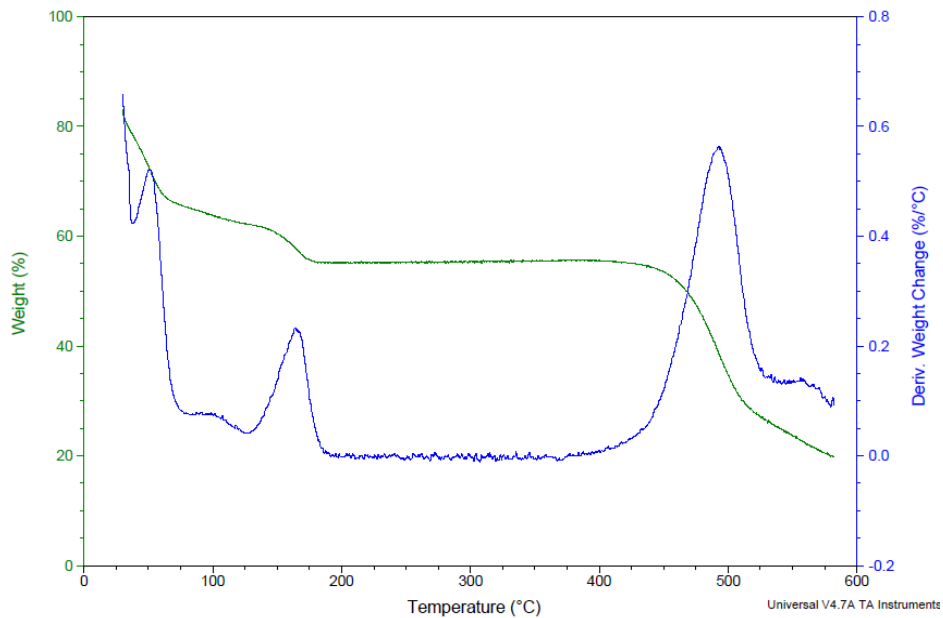
Figure 27: UV-Vis graph of IRMOF-9 measuring the release of linker.

Afterwards TGA is used to correct the weight of the MOF by removing any residual guest or solvent molecule from the calculation. TGA is a method of thermal analysis where the mass of a sample is measured over time as a function of temperature change. With this one could measure the thermal decomposition of a MOF. Thermal decomposition is a point where at a certain temperature a substance chemically decomposes and volatilizes, for IRMOF-9 this temperature is a little after 425 °C, but before that the TGA graph levels off, at that point IRMOF-9 is devoid of all moisture and its guest molecule, normally DMF, is removed leaving only the cage. IRMOF-10 on the other hand does not level off and steadily decomposes until it completely breaks down (**Figure 28**).

Sample: IRMOF-9
Size: 1.4130 mg
Method: Ramp

TGA

File: C:\...TGA\Joseph Strozier\IRMOF-9.001
Operator: AE ER unknown A
Run Date: 01-Dec-2017 11:23
Instrument: TGA Q50 V20.10 Build 36



Sample: JS-70 sample 5 A
Size: 6.7710 mg
Method: 50-600

TGA

File: C:\...JS-70 sample 5 A
Operator: Joe Stro
Run Date: 22-Aug-03 00:24

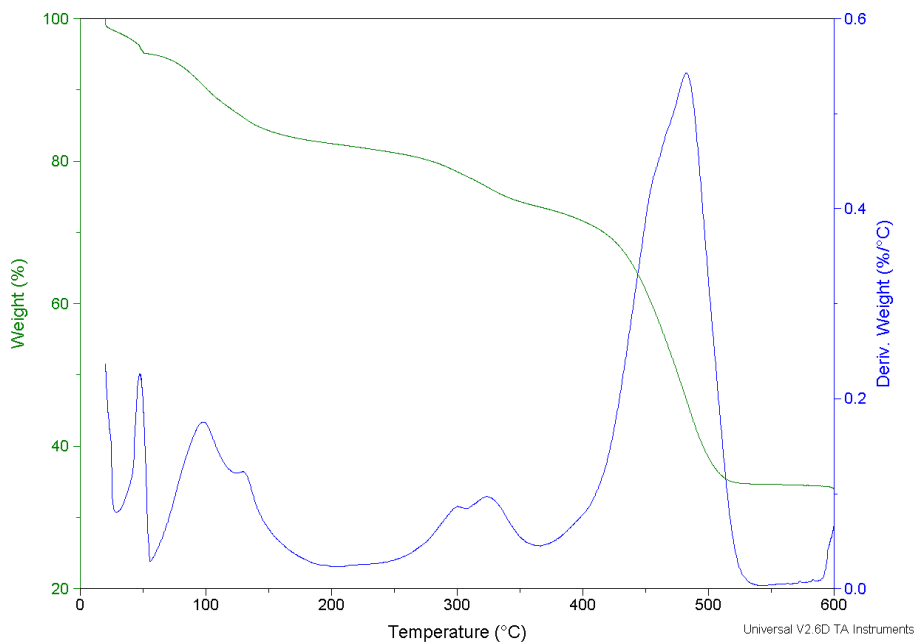


Figure 28: TGA of IRMOF-9 (top) with a TGA of IRMOF-10 (bottom)

At that level off point one can figure out the percentage of IRMOF-9 is composed of DMF and subtract that percentage from the total. After 24 hours of reaction time there is a 40% decrease in weight between IRMOF-9 and IRMOF-10 (**Table 1**). Additionally, if IRMOF-9 is exposed to the deinterpenetration conditions for a whole week then more weight loss (50-90%) is observed (Table 2).

Weight of MOF (g)	TGA weight (Before) (g)	Weight of MOF (open) (g)	TGA weight (after) (g)	Change (g)	% weight loss
0.0385	0.0246	0.0276	0.0220	-0.0164	-42.6
0.0315	0.0201	0.0237	0.0189	-0.0125	-39.8
0.0512	0.0327	0.0389	0.0283	-0.0228	-44.5
0.0405	0.0259	0.0294	0.0238	-0.0166	-41.2

Table 1 Shows the % weight loss in the conversion of IRMOF-9 to IRMOF-10 in 24 hours

Weight of MOF (g)	TGA weight (Before) (g)	Weight of MOF (open) (g)	TGA weight (after) (g)	Change (g)	% weight loss
0.0254	0.0205	0.0074	0.00666	-0.0187	-73.7
0.285	0.0230	0.0179	0.0141	-0.0143	-50.3
0.0401	0.0320	0.022	0.0193	-0.00207	-51.7
0.0463	0.0370	0.0056	0.00453	-0.0417	-90.2
0.0402	0.0321	0.194	0.0176	-0.0227	-56.5

Table 2 shows the % weight loss in the conversion of IRMOF-9 to IRMOF-10 in a week.

Research then shifted to measuring the zinc content in IRMOF-9 to obtain a more thorough understanding of the amount of zinc that was residing inside IRMOF-9. The first step in determining the zinc content was to quantify the amount of 4,4'-biphenyldicarboxylate that resides inside of IRMOF-9. Dried IRMOF-9 that has been weight corrected via TGA is measured in a 4 mL vial and then digested in 1M NaOD, next THF is added to the 4 mL vial with gentle mixing. The vial is then placed in a Nuclear Magnetic Resonance (NMR) tube and a proton NMR is run. While THF wasn't the optimal solvent to use, its NMR signal would not overlap with 4,4'-biphenyldicarboxylic acid. Using 4,4'-biphenyldicarboxylic acid's NMR signal we can then quantify how much of the linker was added by taking the millimole amount of THF and dividing by THF's relative NMR signal when compared to 4,4'biphenyldicarboxylic acid will give you the millimole amount for 4,4'biphenyldicarboxylic acid.

$$\frac{\text{mmol of THF}}{\text{THF relative's NMR signal}} = \text{mmol of linker}$$

You would then take that number and multiply it by the formula weight of the linker to get the observed amount of 4,4'-biphenyldicarboxylic acid in IRMOF-9.

$$\text{mmol of Linker} * \text{formula weight of Linker} = \text{observed amount of Linker}$$

The observed amount of linker is then divided by the theoretical value and the percentage is the amount of linker that is in IRMOF-9.

$$\frac{\text{Observed amount of Linker}}{\text{Theoretical value of Linker}} * 100 = \text{Amount of linker in IRMOF} - 9$$

Next was finding the amount of zinc that was in IRMOF-9. Dried IRMOF-9 that has been weight corrected via TGA is measured in a 4 mL vial and then digested in 1M NH₄OH. A set of zinc standards ranging from 20 ppm to 100 ppm in increments of 20 are made as standards. 10 uL of the digested MOF is diluted up to 10 mL and is ran against the standards to see where it lies. In both cases, quantifying the linker and zinc content of IRMOF-9, the results were inconclusive. It was difficult to obtain reproducible data. In some cases the amount observed would be higher/lower than what could theoretically be observed with values for percent zinc/linker being very sporadic due to this outcome we moved away from this experiment.

MOF-14/MOF-143



Figure 29: MOF-14
copper paddlewheel
SBU

We then moved to see if that same dissolution of a framework would take place in the MOF-14 framework with the copper paddlewheel SBU (**Figure 29**). MOF-14 is a doubly interpenetrated MOF with a copper paddlewheel SBU synthesized from copper nitrate Cu(NO₃)₂, with the linker being made from 1,3,5 benzene tribenzoic acid (H₃BTB). Despite being interpenetrated the void space inside MOF-14 can accommodate a sphere that is ~ 16.4 Å in diameter which is larger than non-interpenetrated MOF-5. It also has a surface area of ~ 1502 m²/g. MOF-14 was synthesized from literature, taking Cu(NO₃)₂ and H₃BTB and dissolving them in a mixture of ethanol, DMF, water,

and pyridine, which was then heated at 65 °C for 24 hours, this results in the formation of light blueish-green cubic crystals.³²

Using the same method to convert IRMOF-9 to IRMOF-10, Et₄NBr/DCM in DMF for 24 hours, MOF-14 was deinterpenetrated to MOF-143. MOF-14 and its non-interpenetrated

MOF-14 vs MOF-143

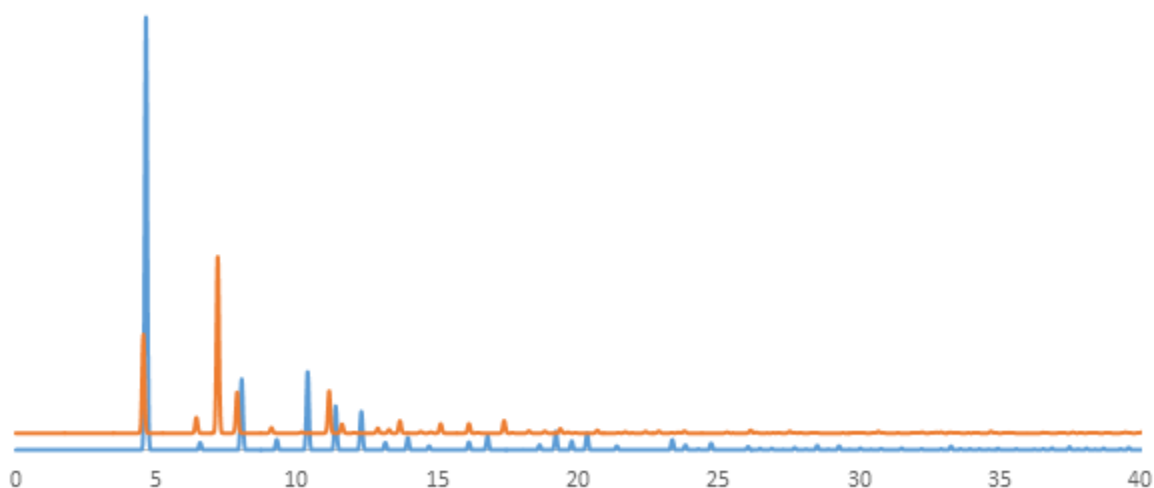


Figure 30: Calculated PXRD patterns of MOF-14 (blue) and MOF-143 (orange)

form MOF-143 also have similar PXRD patterns, so a way to differentiate them aside from powder was needed (**Figure 30**). Using Reichardt's dye we decided to replicate the MOF dyeing experiments that were previously performed.

Timed experiments were ran where MOF-14 crystals were left to deinterpenetrate for every hour, up to five hours (**Figure 31**). The reaction was then arrested by washing with DMF and then treated with a Reichardt's dye/DMF solution to measure the dye uptake.

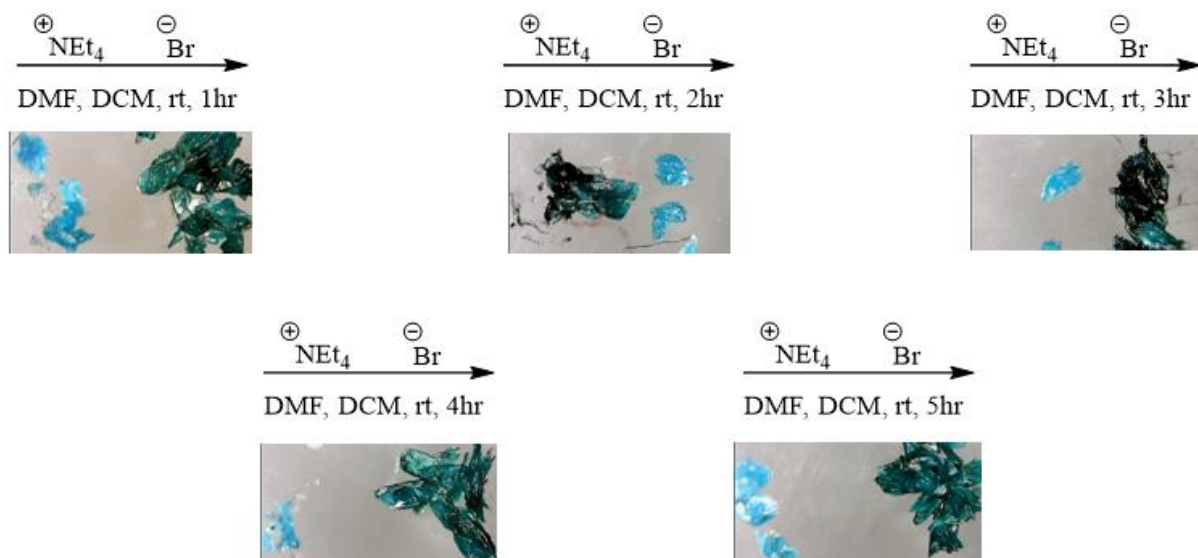


Figure 31: Timed deinterpenetrations from 1 hour to 5 hours. Green crystal is MOF-143 dyed with Reichart's dye, blue crystal is MOF-14

The important takeaway from **Figure 31** is that at every hour the MOF is fully dyed. In fact even as is synthesized MOF-14 is able to incorporate dye from Reichardt's dye without being deinterpenetrated (**Figure 32**). The reason most likely for this would be that the aperture for MOF-14, even though interpenetrated, is large enough to for Reichardt's dye fit inside its opening.

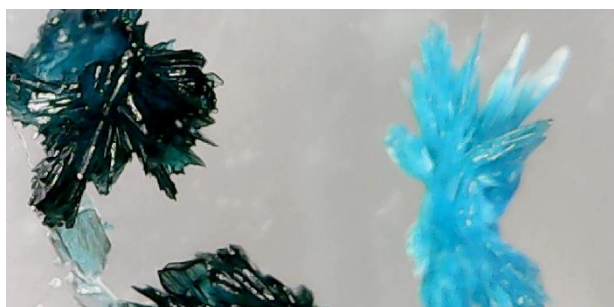


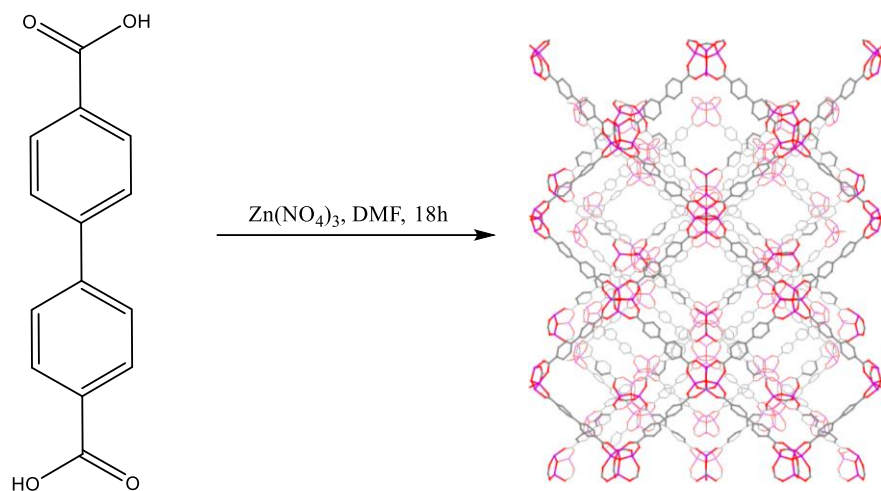
Figure 32: As synthesized MOF-14 (right) and MOF-14 dyed with Reichardt's dye (left)

Conclusion

To summarize, I have studied the IRMOF-9 to IRMOF-10 transformation and have learned the following: despite the two IRMOFs having similar PXRD patterns there are a few ways to differentiate between the two. Through the use of dyes it can be noted that once the diameter of a dye is large enough it will fail to be incorporated into IRMOF-9 due to the pore aperture. IRMOF-9/-10 can be separated by density. IRMOF-9 is the doubly interpenetrated form of IRMOF-10 as such it has a higher density and will sink when placed in a mixture of $\text{CH}_2\text{Cl}_2:\text{CHCl}_3:\text{CH}_2\text{BrCl}$ while IRMOF-10 will float. The TGA curve for IRMOF-10 continuously degrades as the temperature rises where as IRMOF-9 is thermally stable until a temperature greater than $425\text{ }^\circ\text{C}$ is achieved. Although there are multiple ways of synthesizing IRMOF-9 they all behave the same under deinterpenetration/dyeing conditions. Through testing the timing of deinterpenetration it was found there is partial dissolution of the framework with complete dissolution at 5 hours. Although a single crystal of IRMOF-10 was not obtained I have found a reliable method to determine if IRMOF-10 has been obtained, I believe that with further refinement of the deinterpenetration method a single crystal of IRMOF-10 can be obtained.

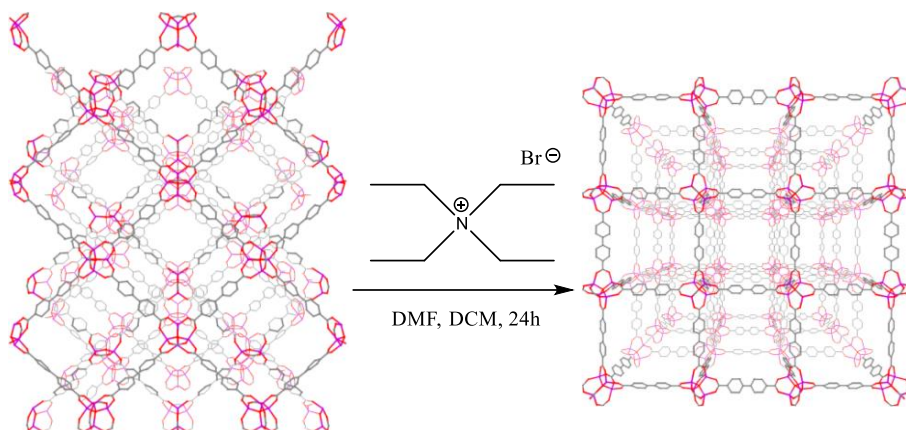
Experimental

Synthesis of IRMOF-9



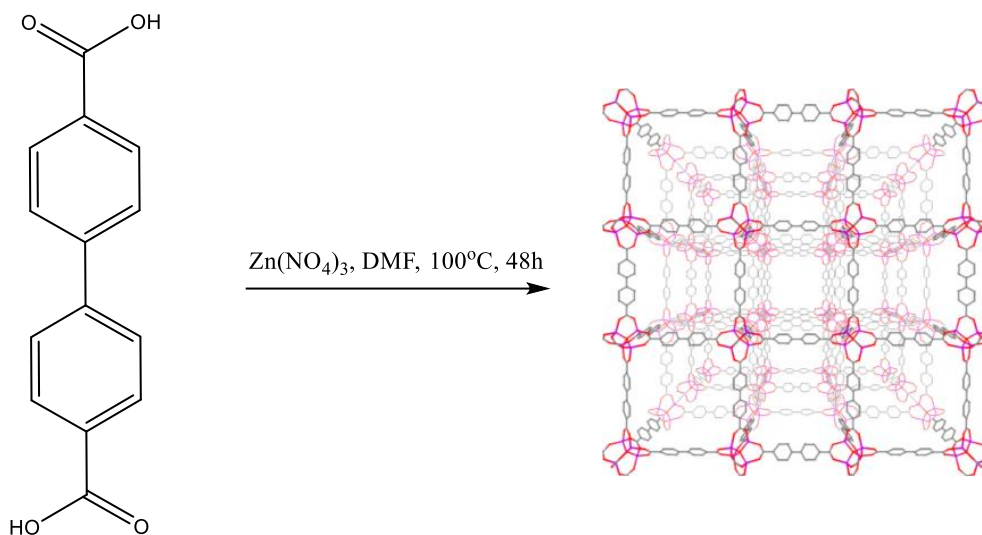
To a 250 mL beaker charged with DMF (100 mL) was added $\text{Zn}(\text{NO}_3)_2 \cdot 6\text{H}_2\text{O}$ (1.8 g, 6.1 mmol) and 4,4'-biphenyldicarboxylic acid (0.3 g, 1.2 mmol). A stir bar was added and the mixture stirred for 15 minutes. The solution was then filtered through a GE 25 mm PVDF syringe filter (0.45 μm) in 6 mL portions, into 16 individual 20 mL scintillation vials. The vials were capped with Teflon-lined caps and then placed in a 100 $^\circ\text{C}$ oven for 18h. At this time the vials were removed from the oven and allowed to ambiently cool to room temperature. The crystalline solids were then combined and washed with fresh DMF (3 x 10 mL). The liquid was decanted and the solids were characterized by PXRD, dye test (described below), density test (described below), TGA, and NMR. Then the MOF is dried (described below).

Conversion of IRMOF-9 to IRMOF-10



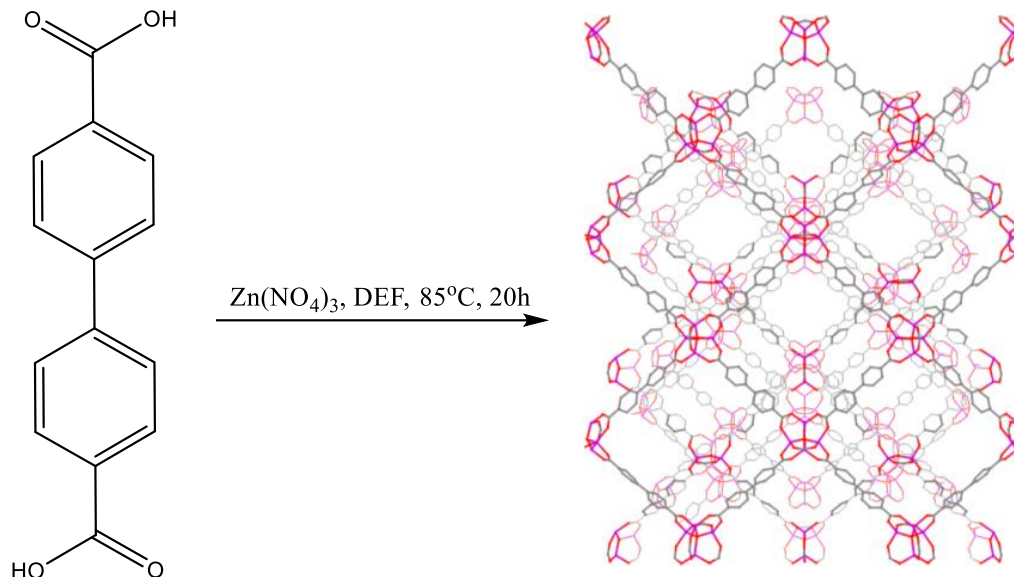
To a 20 mL scintillation vial was added 30 mg of IRMOF-9, and charged with 1:1 (v/v) mixture of 1.5 mL of DMF, and 1.5 mL of a 0.32 M solution of TEABr (0.96 mmol) in DCM. The vial was then allowed to agitate on an orbital shaker at 75 rpm at room temperature for 24 hours. At this time the vial was removed from the shaker, and all liquids were decanted off. The remaining solids were then washed with fresh DMF (3 x 3 mL). The liquid was decanted and the solids were characterized by PXRD, dye test (described below), density test (described below), TGA, and NMR and ICP-MS of the digested MOF.

Synthesis of IRMOF-10 (Hupps)³⁰



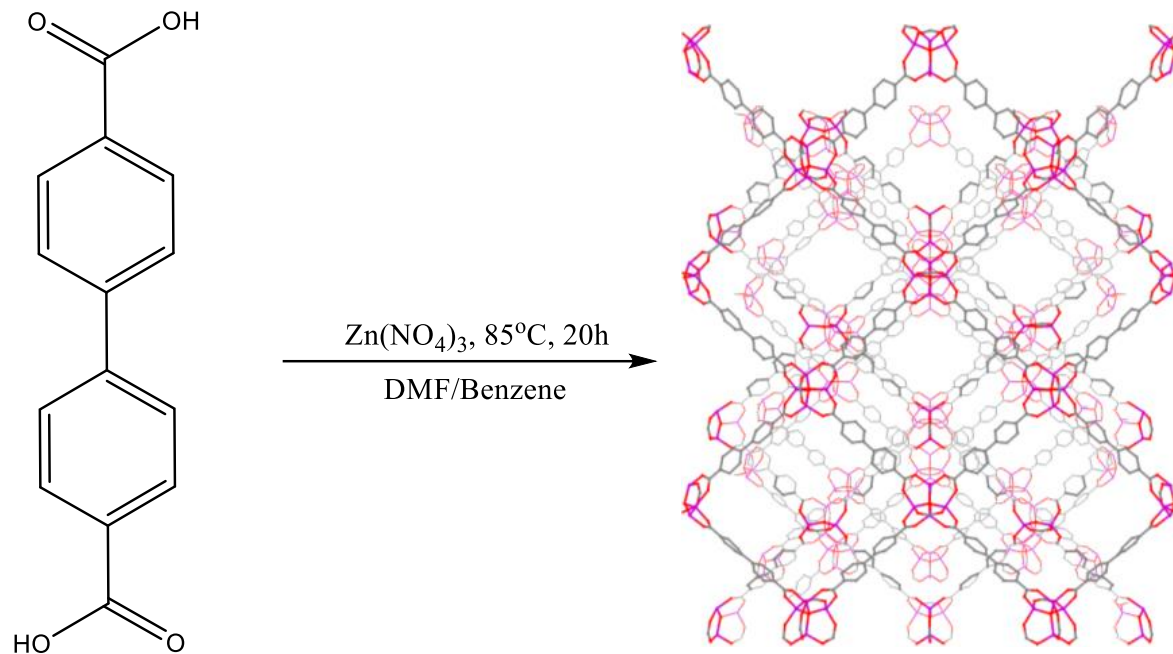
To a 400 mL beaker charged with DMF (266 mL) was added $\text{Zn}(\text{NO}_3)_2 \cdot 6\text{H}_2\text{O}$ (0.7 g, 2.3 mmol) and 4,4'-biphenyldicarboxylic acid (0.1 g, 0.4 mmol). The mixture is sonicated for 15 minutes, the solution was then filtered through a GE 25 mm PVDF syringe filter (0.45 μm) in 6 mL portions, into 44 individual 20 mL scintillation vials. The vials were capped with Teflon-lined caps and then placed in a 100 °C oven for 48h. At this time the vials were removed from the oven and allowed to ambiently cool to room temperature. The crystalline solids were then combined and washed with fresh DMF (3 x 10 mL). The liquid was decanted and the solids were characterized by PXRD, dye test (described below), density test (described below), and TGA. Then the MOF is dried (described below).

Synthesis of IRMOF-9 Method #1



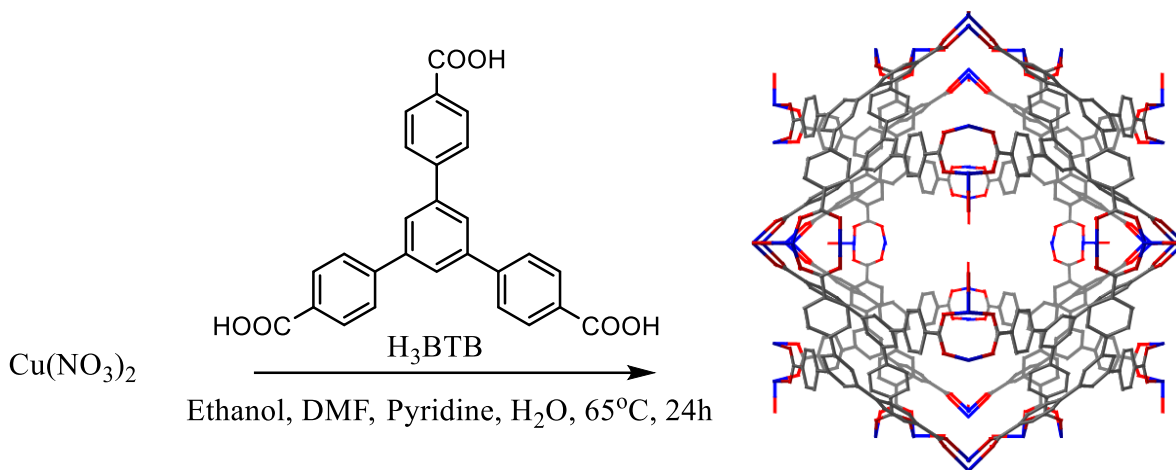
To a 250 mL beaker charged with DEF (45 mL) was added $\text{Zn}(\text{NO}_3)_2 \cdot 6\text{H}_2\text{O}$ (0.55 g, 1.8 mmol) and 4,4'-biphenyldicarboxylic acid (0.40 g, 1.6 mmol). The mixture was sonicated for 15 minutes, the solution was then filtered through a GE 25 mm PVDF syringe filter (0.45 μm) in 6 mL portions, into 8 individual 20 mL scintillation vials. The vials were capped with Teflon-lined caps and then placed in an 85 °C oven for 20h. At this time the vials were removed from the oven and allowed to ambiently cool to room temperature. The crystalline solids were then combined and washed with fresh DMF (3 x 10 mL). The liquid was decanted and the solids were characterized by PXRD, dye test (described below), density test (described below), TGA, and NMR. Then the MOF is then dried (described below).

Synthesis of IRMOF-9 Method #2



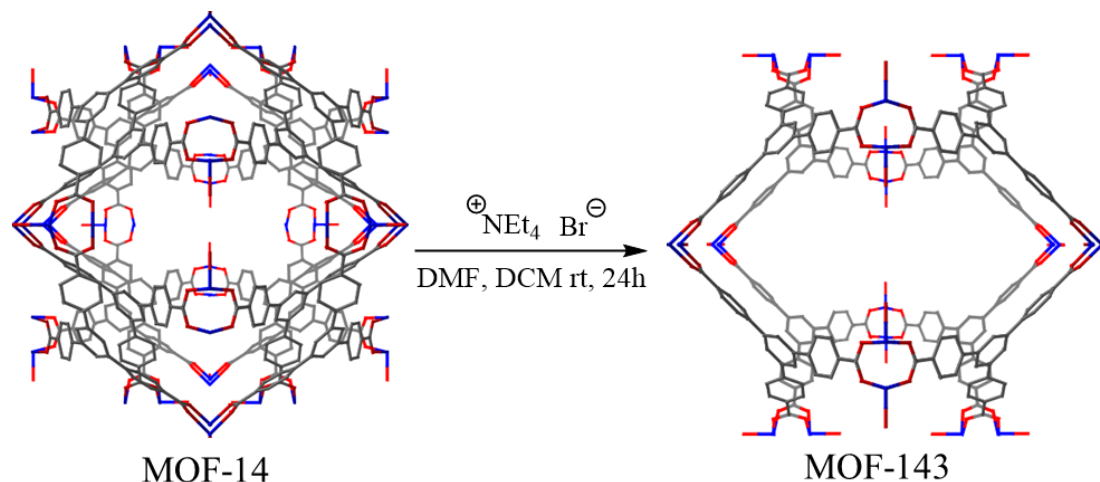
To a 250 mL beaker charged with DMF (20 mL) and benzene (20 mL) was added $\text{Zn}(\text{NO}_3)_2 \cdot 6\text{H}_2\text{O}$ (0.650g, 2.2mmol) and 4,4'-biphenyldicarboxylic acid (0.075 g, 0.31 mmol). The mixture was sonicated for 15 minutes, the solution was then filtered through a GE 25 mm PVDF syringe filter ($0.45 \mu\text{m}$) in 6 mL portions, into 7 individual 20 mL scintillation vials. The vials were capped with Teflon-lined caps and then placed in an 85°C oven for 20h. At this time the vials were removed from the oven and allowed to ambiently cool to room temperature. The crystalline solids were then combined and washed with fresh DMF (3 x 10 mL). The liquid was decanted and the solids were characterized by PXRD, dye test (described below), density test (described below), TGA, and NMR. Then the MOF is dried (described below).

Synthesis of MOF-14³¹



To a 20 mL scintillation vial charged with a mixture of DMF/NMP/pyridine (5 mL, 5 mL, 0.4 mL) was added $\text{Cu}(\text{NO}_3)_2$ (0.06 g, 0.3mmol) and 1,3,5 benzene tribenzoic acid (0.021 g, 0.048 mmol). The mixture is then sonicated for 3 minutes, the solution was then filtered through a GE 25 mm PVDF syringe filter (0.45 μm) into 1 individual 20 mL scintillation vial. The vial was capped with a Teflon-lined cap and placed in an 85°C oven for 48 hours. At this time the vials were removed from the oven and allowed to ambiently cool to room temperature. The crystalline solids were then combined, washed and stored with fresh DMF (3 x 10 mL), the liquid was decanted and the solids were characterized by PXRD and dye test (described below).

Conversion of MOF-14 to MOF-143



To a 20 mL scintillation vial charged with 30 mg of MOF-143, and a 1:1 (v/v) solution of 1.5 mL of DMF, and a 1.5 mL of a 0.32 M solution of TEABr (0.96 mmol) in DCM. The vial was then allowed to agitate on an orbital shaker at 100 rpm at room temperature for 24 hours. At this time the vial was removed from the shaker, and all liquids were decanted off. The remaining solids were then washed with fresh DMF (3 x 3 mL), the liquid was decanted and the solids were characterized by PXRD and dye test (described below).

Drying method for IRMOF-9/IRMOF-10

0.5 g of IRMOF-9/IRMOF-10 is loaded into a 20 mL scintillation vial fitted with a vacuum adapter and is pumped on under reduced pressure, ~0.5 torr, for 24 hours at room temperature.

Dying of IRMOF-9/IRMOF-10 with Reichardt's dye

To a 4 mL scintillation vial was added MOF (15 mg) and a 0.001 mM solution of Reichardt's dye in DMF (1.0 mL). After 24 hours, the crystals were removed from the solution and observed via optical light microscopy.

Dying of IRMOF-9/IRMOF-10 with Rhodamine B

To a 4 mL scintillation vial was added MOF (15 mg) and a 0.001 mM solution of Rhodamine b in DMF (1.0) for 24 hours. After 24 hours, the crystals are removed from the solution and observed using optical light microscopy.

Dying of MOF-14/MOF-143 with Reichardt's dye

To a 4 mL scintillation vial was added MOF (30 mg) and 0.001 mM solution of Reichardt's dye in DMF for 24 hours. After 24 hours, the crystals are removed from solution observed using optical light microscopy.

Sample preparation for ICP-MS analysis (zinc quantification)

A known quantity¹ (2-5 mg) of dried MOF is digested in conc. NH_4OH (1 mL). The digestion solution is treated with 10 μL of 1000 ppm yttrium standard and then is volumetrically diluted with deionized water to 10 mL. The solution is then transferred into a 15 mL plastic conical centrifuge tube that has been pretreated with dilute HNO_3 for 24 hours. The sample is then analyzed via ICP-MS as described in the general techniques section.

Sample preparation for H_2BDC quantification by ^1H NMR

A known quantity² (5-10 mg) of dried MOF is digested in 1M NaOD (1 mL) solution, prepared by dissolving NaOH in D_2O . Next THF (20 μL) is added as a standard to the sample which is then sonicated for 1 minute. The sample is then analyzed by ^1H NMR as described in the general techniques section

Separation of IRMOF-9/10 via density²⁸.

To a 20 mL scintillation vial charged with 15 mL of a 4:5:26 (b/v) solution of CH_2Cl_2 : CHCl_3 : CH_2BrCl was added MOF. Any sample that remained floating was filtered off the top. The remaining solids that sank to the bottom were isolated after the remaining liquid was decanted. Both the floating and sinking solids were characterized by PXRD, dye test, TGA, and NMR and ICP-MS of the digested MOF

¹ Note the mass of the weighed MOF is corrected by subtracting the mass of residual solvent as determined using thermogravimetric analysis.

² Note the mass of the weighed MOF is corrected by subtracting the mass of residual solvent as determined using thermogravimetric analysis.

UV-Vis absorbance experiment

To a quartz cuvette charged with a 0.0032M solution of Et₄NBr in 1:1 DMF:DCM (b/v) is added dried IRMOF-9 (2 mg). UV-vis readings are then taken every 2 minutes for five hours.

References

1. Spagnolo, L. L.; El-Hankari, S.; Bradshaw, D. *Chem. Soc. Rev.* **2014**, *43*, 5431.
2. Eddaoudi, M.; Kim, J.; Rosi, N.; Vodak, D.; Wachter, J.; O’Keeffe, M.; Yaghi, O. M.. *Science* **2002**, *295*, 469–472.
3. Latrochi, M.; Surbie, S.; Serre, C.; Mellot-Draznieks, C; Llewellyn, P.L.; Lee, J.H.; Chang, J. S.; Jhung, S. H.; Ferey, G. *Angew. Chem. Int. Ed.* **2006**, *45*, 8227-8231
4. Rosi, N. L.; Eckert, J.; Eddaoudi, M.; Vodak, D. T.; Kim, J.; O’Keeffe, M.; Yaghi, O. M. *Science* **2003**, *300*, 1127–1129.
5. Chen, B.; Liang, C.; Yang, J.; Contreras, D. S.; Clancy, Y. L.; Lobkovsky, E. B.; Yaghi, O. M.; Dai, S. A. *Angew. Chem., Int. Ed.* **2006**, *45*, 1390–1393.
6. Li, J.-R.; Kuppler, R. J.; Zhou, H.-C. *Chem. Soc. Rev.* **2009**, *38*, 1477–1504.
7. Henschel, A.; Gedrich, K.; Kraehnert, R.; Kaskel, S. *Chem. Commun.* **2008**, 4192–4194.
8. Wang, C.; Zheng, M.; Lin, W. J. *Phys.Chem. Lett.* **2011**, *2*, 1701–1709.
9. Della Rocca, J.; Liu, D.; Lin, W. *Acc. Chem.Res.* **2011**, *44*, 957–968.
10. Horcajada, P.; Serre, C.; Vallet-Regi, M.; Sebban, M.; Taulelle, F.; Ferey, G. *Angew. Chem., Int. Ed.* **2006**, *45*, 5974–5878.
11. Horcajada, P.; Gref, R.; Baati, T.; Allan, P. K.; Maurin, G.; Couvreur, P.; Ferey, G.; Morris, R. E.; Serre, C. *Chem. Rev.* **2012**, *112*, 1232–1268.
12. Silva, C. G.; Corma, A.; Garcia, H. J. *Mater. Chem.* **2010**, *20*, 3141–3156.
13. Li, H.; Eddaoudi, M.; O’Keeffe, M.; Yaghi, M. O. *Nature.* **1999**, *402*, 276.
14. Li, H.; Wang, K.; Sun, Y.; Lollar, T. C.; Li, J.; Zhou, H. *Materials Today.* **2018**, *21*, 108-121
15. Ritesh, H.; Nivedita, S.; Tapas, K. M. *Materials Today.* **2015**, *18*, 97-116

16. R. Vaidhyanathan, S. Iremonger, G. Shimizu, P. Boyd, S. Alavi and T. Woo, *Science*, **2010**, 330, 650.
17. L. Pan, D. H. Olson, L. R. Ciemnomolonski, R. Heddy and J. Li, *Angew. Chem., Int. Ed.*, **2006**, 45, 616
18. Yang, S.; Lin, X.; Lewis, W.; Suyetin, M.; Bichoutskaia, E.; Parker, E. J.; Tang, C. C.; Allan, R. D.; Rizkallah, J. P.; Hubberstey, P. Champness, R. N.; Thomas, K. M.; Blake, J. A.; Schroder, M. *Nature*. **2012**, 710-716.
19. Shengqian, M.; Xi-Sen, W.; Daqiang, Y.; Hong-Cai, Z. *Angew. Chem. Int. Ed.* **2008**, 47, 4130-4133
20. Farha, K. O.; Malliakas, D. C.; Kanatzidis, G. M.; Hupp, T. J. *J. Am. Chem. Soc.* **2010**, 132, 950-952.
21. Maji, K. T.; Matsuda, R.; Kitagawa, S.; *Nature*. **2007**, 142-148.
22. H.-L. Jiang, Y. Tatsu, Z.-H. Lu, Q. Xu, *J. Am. Chem. Soc.* **2010**, 132, 5586.
23. S. Ma, D. Sun, M. Ambrogio, J.A. Fillinger, S. Parkin, H.-C. Zhou, *J. Am. Chem. Soc.* **2007**, 129, 1858;
24. Choi, B. S.; Furukawa, H.; Nam, J. H.; Jung, D.; Jhon, H.Y.; Walton, A.; Book, D.; O’Keeffe, O. M.; Yaghi, M. O.; and Kim, J. *Angew. Chem. Int. Ed.* **2012**, 51, 8791 – 8795
25. J. L. C. Rowsell, O. M. Yaghi, *J. Am. Chem. Soc.* **2006**, 128, 1304 – 1315;
26. Zhang, J.; Wojtas, L.; Larsen, W. R.; Eddaoudi, M.; Zaworotko, M. *J. AM. CHEM. SOC.* **2009**, 131, 17040–17041
27. Jiang, H-L.; Makal, T. A.; Zhou, H-C. *Coordination Chemistry Reviews.* **2013** 257 2232–2249
28. Schnobrich, J.K.; Koh, K. Sura, K. N.; Matzger, A. J. *Langmuir* **2010**, 26, 8, 5808-5814
29. M. K. Bellas, J. J. Mihaly, M. Zeller, D. T. Genna, *Inorg. Chem.* **2017**, 56, 950–955
30. Farha, O. K.; Mulfort, K. L.; Thorsness, A. M.; Hupp, J. T. *J. Am. Chem. Soc.* **2008**, 130, 8598

31. K. Koh,; A.G Wong-Foy,; A.J. Matzger. *Chem. Commun.*, **2009**, 6162–6164
32. Yaghi, O.M; Eddaoudi, M; Li, H; Kim, J; Rosi, N. Isoreticular metal-organic frameworks, process for forming the same, and systematic design of pore size and functionality therein, with application for gas storage. US 2003/0004364 A1, 2003
33. Banglin, C.; Eddaoudi, M.; Hyde, S. T.; O’Keeffe, M.; Yaghi, O. M.. *Science* **2001**, 291, 469–472